The Cryosphere Discuss., https://doi.org/10.5194/tc-2017-265
Manuscript under review for journal The Cryosphere
Discussion started: 12 December 2017

The Cryosphere Discussions
Open Access
EGU

Mercury in arctic tundra snowpack: temporal and spatial concentration patterns and trace-gas exchanges

Yannick Agnan[1,2], Thomas A. Douglas[3], Detlev Helmig[4], Jacques Hueber[4], Daniel Obrist[5,2]

[1]Milieux Environnementaux, Transferts et Interactions dans les hydrosystèmes et les Sols (METIS), UMR 7619, Sorbonne Universités UPMC–CNRS–EPHE, 4 place Jussieu, F-75252 Paris, France
[2]Division of Atmospheric Sciences, Desert Research Institute, Reno, Nevada 89523, USA
[3]US Army Cold Regions Research and Engineering Laboratory, PO Box 35170, Fort Wainwright, Alaska 99709, USA
[4]Institute of Arctic and Alpine Research, University of Colorado, Boulder, Colorado 80309, USA
[5]Department of Environmental, Earth, and Atmospheric Sciences, University of Massachusetts, Lowell, MA 01854, USA

Correspondence to: Yannick Agnan (yannick.agnan@biogeochimie.fr) and Daniel Obrist (daniel_obrist@uml.edu)

Abstract. In the Arctic, the snowpack forms the major interface between atmospheric and terrestrial mercury (Hg) cycling, a global pollutant. In this study, we investigated Hg dynamics in an interior arctic tundra snowpack in northern Alaska during two snow seasons. Using a snow tower system and soil wells to monitor trace gas exchange of Hg, we observed consistent concentration declines of gaseous elemental Hg (Hg^0_{gas}), the volatile form of Hg, from the atmosphere to the snowpack to soils. This indicates a sink of Hg^0_{gas} in tundra soils. There was no evidence of photochemical reduction of Hg^{II} to Hg^0_{gas} in the tundra snowpack, unlike in temperate snowpacks, with the exception of short periods during late winter. We consistently measured low concentrations of both total (Hg_{tot}) and dissolved (Hg_{diss}) Hg in the tundra snowpack throughout two years (generally <1.0 and 0.3 ng L^{-1}, respectively). Chemical tracers showed that Hg was mainly associated with local mineral dust and regional marine sea spray inputs. Mass balance calculations of Hg show that the snowpack represents a very small reservoir of Hg, resulting in low inputs during snowmelt (<30 ng m^{-2} for Hg_{diss}). The interior arctic snowpacks may be negligible sources of Hg in the Arctic.

1 Introduction

Mercury (Hg) is a neurotoxic pollutant of worldwide importance that is transported over long distances in the atmosphere as gaseous elemental Hg (Hg^0_{gas}) and thus reaches remote environments (Cobbett et al., 2007; Driscoll et al., 2013; Sprovieri et al., 2010). In the Arctic, modern atmospheric Hg deposition has increased about three-fold from Hg pre-industrialized background levels (Fitzgerald et al., 2005), similar to increases observed across temperate areas. The increase in Hg loading has led to vulnerability of polar ecosystems to Hg contamination due to detrimental impacts to wildlife and humans, in particular through biomagnification processes across trophic levels (Atwell et al., 1998).

Representing about 26% of the global land surface area, polar regions are unique environments with specific physical, chemical, and biological processes (Douglas et al., 2012). In particular, most of the northern latitudes are covered by a laterally continuous snowpack during long periods of the year. In the Alaskan tundra, the surface snow cover is present about two thirds

of the year (Cherry et al., 2014). The snowpack hence forms a critical interface between the arctic atmosphere, tundra ecosystems, and underlying tundra soils. Trace gas exchanges between the atmosphere and the tundra are modulated by sinks and sources below and within snowpack, by snow diffusivity, snow height, and snow porosity (Dominé and Shepson, 2002; Lalonde et al., 2002; Monson et al., 2006). The snowpack accumulates nutrients, pollutants, and impurities that are deposited by snowfall and dry deposition processes, all of which can subsequently be transported to underlying ecosystems during snowmelt (Bergin et al., 1995; Uematsu et al., 2000).

The snowpack plays an important role for the cycling of Hg, including for atmospheric deposition, photochemical oxidoreduction reactions, and associated phase changes between solid and gaseous Hg that can volatilize Hg to the atmosphere (Douglas et al., 2008; Faïn et al., 2013; Mann et al., 2014; Steffen et al., 2013). In particular, many temperate and arctic studies have shown that the snowpack can serve as sinks or sources of Hg^0_{gas}, whereby photochemical reduction of snow-bound Hg^{II} can produce Hg^0_{gas} and oxidation processes can reversely scavenge atmospheric Hg^0_{gas} in snow (Faïn et al., 2013; Lalonde et al., 2002; Mann et al., 2011). Photochemical reactions occur primarily in the top 10 cm of the snowpack where sunlight radiation transmits and is absorbed and scattered by snow crystals (Faïn et al., 2007; King and Simpson, 2001). The degree of photochemical production of Hg^0_{gas} and subsequent atmospheric re-volatilization from the snowpack can be very significant, as shown in temperate snowpacks with strong recurring daytime atmospheric emissions of Hg^0_{gas} throughout the winter season (Faïn et al., 2013). In global models, snowpack Hg^0_{gas} emissions have been incorporated to account for ~50% of all snowpack Hg (Corbitt et al., 2011). The reverse process—oxidation of Hg^0_{gas} to Hg^{II}—, has also been proposed to occur in the dark snowpack deeper in the snow profile (Faïn et al., 2007, 2013; Mann et al., 2015), resulting in concentration declines of Hg^0_{gas} with depth in the snowpack. To our knowledge, no direct measurement of snowpack Hg^0_{gas} dynamics, however, is available in the field in the interior arctic snowpack.

In the Arctic and Antarctic, Hg cycling also is affected by atmospheric Hg depletion events (AMDEs) which are observed primarily in the springtime along coastal locations (Dommergue et al., 2010; Schroeder et al., 1998; Steffen et al., 2008). During AMDEs, atmospheric Hg^0_{gas} concentrations fluctuate strongly due to atmospheric conversion of Hg^0_{gas} to oxidized Hg^{II}. Because Hg^{II} is subject to faster deposition (Schroeder and Munthe, 1998; Selin, 2009), AMDEs result in large amounts of Hg temporarily deposited from the atmosphere to the arctic ecosystems. AMDEs are considered to be initiated by halogens (Brooks et al., 2008; Obrist et al., 2011; Steffen et al., 2008), such as bromine and chlorine radicals released from sea salt by photochemical processes (Simpson et al., 2007). AMDEs have been mainly observed along the coasts, e.g., at Barrow in Alaska (Douglas et al., 2008), Alert in Canada (Steffen et al., 2002), Ny-Ålesund in Svalbard (Ferrari et al., 2008), McMurod in Antarctica (Brooks et al., 2008), as well as directly over the sea ice (Moore et al., 2014; Nerentorp Mastromonaco et al., 2016). The impacts of AMDEs at inland sites is reduced with increasing distance from the coast (Douglas and Sturm, 2004; Obrist et al., 2017; Van Dam et al., 2013).

The objectives of this study were to characterize Hg dynamics in the inland arctic snowpack at Toolik Field Station and along a 170-km transect between this site and the arctic coast. For the first time, we comprehensively linked trace gas fluxes of Hg^0_{gas} in interstitial snow air with the seasonal development of total Hg (Hg_{tot}) and dissolved Hg (Hg_{diss}) bound in the snowpack to

assess conversions between volatile and solid Hg in the arctic snowpack. We specifically aimed to assess: (1) temporal and vertical Hg^0_{gas} patterns to quantify exchanges of Hg^0_{gas} in the atmosphere–snowpack–soil continuum; (2) impacts of springtime AMDEs on snowpack Hg deposition to and emission from the inland arctic snowpack; (3) temporal and vertical concentration and mass patterns of the snowpack Hg_{tot} and Hg_{diss} to estimate Hg deposition throughout the snow accumulation period and pool of Hg available through snow melt; and (4) relationships of snow Hg concentrations with major ions concentrations and oxygen and hydrogen stable isotopes in precipitation to determine potential origins of Hg contained in the snowpack.

2 Materials and methods

2.1 Study site

Measurements were mainly performed at Toolik Field Station (Alaska, USA) over two full snow cover seasons from October 2014 to May 2016. The research station is located on the north slopes of the Brooks Range (68° 38' N, 149° 36' W) at an elevation of 720 m a.s.l, approximately 200 km south of the Arctic Ocean (Figure 1, orange bullet). The lithology is characterized by glacial till over Cretaceous sedimentary substrates (shale, claystone, siltstone, and sandstone; Alaska Division of Oil and Gas, 2008). The ecotype is classified as an acidic tussock tundra (Shaver and Chapin, 1991) with vegetation composed of scrubby plants (e.g., *Cassiope tetragona* (L.) D.Don, *Arctostaphylos alpinus* (L.) Spreng.), shrubs (e.g., *Betula nana* L., *Salix pulchra* Cham.), tussock grasses (*Carex*), and a variety of mosses and lichens. The mean annual air temperature is −8.5 °C and mean annual precipitation is 312 mm (Cherry et al., 2014). In the two measurement years, the tundra was covered by snow for 236 and 248 days (i.e., 65 and 68% of the year) in the 2014–2015 and 2015–2016 seasons, respectively. Snowpack sampling was also performed along a transect between Toolik and the Arctic Ocean in March 2016 (Figure 1, yellow bullets). The full geographical details are given in Table S1. A total of eight study sites were sampled from south (500 m a.s.l.) to north (20 m a.s.l.). All the sampled sites were characterized by similar ecosystems and lithology (including undifferentiated volcanic Upper Tertiary beds to the north) as described above for Toolik.

2.2 Trace gas in the atmosphere, interstitial snow air, and soil pores

We continuously sampled and analyzed interstitial air of the tundra snowpack at Toolik using a snow tower (Figure S1) as described in detail by Seok et al. (2009) and Faïn et al. (2013). In summary, a snow tower consists of an air inlet manifold placed in the snowpack so sampling of trace gases can be remotely alternated between various snow depths for undisturbed sampling of interstitial snow air throughout an entire snow season. The snow tower used at Toolik consisted of six 60 cm aluminum cross arms mounted at heights of 0, 10, 20, 30, 40, and 110 cm above the ground surface. Two trace gas inlets were mounted to each cross arm allowing vertical sampling of snow interstitial air and subsequent analysis for multiple trace gases, including Hg^0_{gas}, CO_2, and O_3. Each cross arm of the snow tower supported a pair of air inlets fitted with 25 mm syringe filters with 1 µm glass fiber membranes (Pall Life Sciences, Ann Arbor, MI, USA). Perfluoroalkoxy Teflon® tubing with equal lengths (35 m) were directed with a heated conduit to solenoid valves in the laboratory that allowed for sequential sampling of

trace gases at the six different snowpack heights. The snow tower was deployed over the tundra in August of each year prior to the onset of snowfall. When the snow tower was subsequently covered by the accumulating snowpack, this set-up allowed sequentially continuous sampling of snow interstitial air from the adjacent laboratory without any disturbance. Inlets were sampled sequentially, 5 min at a time, resulting in a 30-min sampling cycle. Corresponding trace gas sampling was performed below the snowpack in tundra soils at depths of 10, 20, and 40 cm using Teflon® soil trace gas wells (Obrist et al., 2014, 2017). Atmospheric air sampling was performed using the top snow tower air inlet which always was above the developing snowpack, as well as on a nearby micrometeorological tower at a height of 3.6 m above ground. All interstitial snow, soil pore, and atmospheric inlets were connected by Teflon® tubing and solenoid valves to trace gas monitors in a nearby (10–30 m distance) field laboratory that were operated year-round.

Gaseous Hg^0 concentrations were measured using two Tekran 2537B analyzers (Tekran Instruments Corporation, Toronto, ON, Canada), one for interstitial snow air measurements and the other shared for soil gas and atmospheric measurements. Air sampling was alternated between different snowpack heights every 5 min so that a full sequence of air extraction from the snowpack (six inlet heights) was achieved every 30 min. Interstitial snow, soil pore, and atmospheric measurements continued through the entire winter with only small-time periods of interruptions due to power failures or other technical problems. Additional trace gases were measured along with Hg^0_{gas}, including concentrations of CO_2 using a LI-840A (LI-COR Inc., Lincoln, NE, USA).

2.3 Snow sampling and physical and chemical characterization

2.3.1 Snow sampling

At Toolik, we characterized Hg in the snowpack both over the undisturbed tundra and the adjacent frozen Toolik Lake (within 200 m of the tundra location). Snow pits were sampled on five dates between October and May in the 2014–2015 season, and on four dates between December and June in 2015–2016. For each pit, we vertically excavated snow samples using a stainless-steel snow cutter (RIP 1 cutter 1000 cc), clean latex gloves, and trace metal Nasco Whirl-Pak® (The Aristotle Corporation, Stamford, CT, USA) HDPE plastic bags. We sampled at 10 cm-layer increments from the top to the bottom of the snowpack. Two replicate samples from perpendicular walls of the pit were each pooled together per layer for analysis. Snow height, density, and temperatures were measured for each layer, and frozen snow samples were stored in a cooler before transferring to a −20 °C freezer. Additional sampling of surface snow was performed over the tundra for a total of 17 sampling dates. The top 3 cm of the snowpack was collected in triplicate into Nasco Whirl-Pak® plastic bags using clean latex gloves. Sampling along the south to north transect was performed over two days in March 2016.

2.3.2 Chemical analyses

In the laboratory, we stored snow samples overnight in the Nasco Whirl-Pak® bags at room temperature in the dark, and melted snow samples were subsequently analyzed for Hg. A fraction of snowmelt was directly transferred to 50 mL

polypropylene tubes (Falcon®, Corning Incorporated, Corning, NY, USA) for analysis of Hg_{tot}. For Hg_{diss}, snowmelt water was filtered using 0.45 µm Acrodisc® filter with polyethersulfone membrane (Pall Corporation, Port Washington, NY, USA) into 50 mL Falcon® polypropylene tubes. In addition, filtered meltwater was used in 60 mL high-density polyethylene tubes (VWR®, Radnor, PA, USA) for determination of major cations, anions, and stable isotopes (^{2}H and ^{18}O). Hg_{tot} and Hg_{diss} concentrations were determined using Tekran 2600 cold-vapor atomic fluorescence spectrometry (Tekran Instruments Corporation, Toronto, ON, Canada) using a bromine monochloride (BrCl) digestion and reduction by stannous chloride ($SnCl_2$) following the EPA method 1631 (US EPA, 2002). The detection limits, determined as 3-times the standard deviation of blank samples, averaged 0.08 ng L^{-1}. For statistic purpose, values below the detection limit (DL) were included as 0.5 × DL. Recoveries, determined by 5 ng L^{-1} standards analyzed every 10 samples, averaged between 93 and 107%. Laboratory and field blanks were conducted, and we evaluated any potential metal contamination of the stainless-steel snow cutter by analyzing Milli-Q water in contact with the snow cutter; all these blank determinations were bellow detection limits.

Major cation and anion concentrations were quantified at the U.S. Army Cold Regions Research and Engineering Laboratory's (CRREL) Alaska Geochemistry Laboratory on Fort Wainwright, Alaska with a Dionex ICS-3000 ion chromatograph. An AS-19 anion column and a CS-12A cation column (Dionex Corporation Sunnyvale, California) were used, each with a 10 µL injection volume. A gradient method using potassium hydroxide eluent ranged from 20 to 35 µmol L^{-1} in concentration for anion analyses, while cation analyses used methane sulfonic acid eluent with a concentration of 25 µmol L^{-1} in isocratic mode. The flow rate was 1 mL min^{-1} and the operating temperature was 30 °C. The ion chromatograph was calibrated using standards with a range of values from 0.5 to 50 mg L^{-1}. Repeat analyses of calibration standards from 0.5 to 50 mg L^{-1} yielded a calculated precision for the analyses of ±5%. Peaks were identified using Chromeleon (Dionex) and verified visually.

Stable isotopes of oxygen and hydrogen were also measured at CRREL Alaska using Wavelength-Scanned Cavity Ringdown Spectroscopy on a Picarro L2120i (Sunnyvale, California). Standards and samples were injected into the analyzer for seven separate analyses. Results from the first four injections were not used to calculate the stable isotope values to eliminate internal system memory. The mean value from the final three sample injections was used to calculate the mean and standard deviation value for each sample. Values are reported in standard per mil notation. Repeated analyses of five internal laboratory standards representing a range of values spanning the samples analyzed and analyses of SMOW, GISP, and SLAP standards (International Atomic Energy Agency) were used to calibrate the analytical results. Based on thousands of these standards analyses and of sample duplicate analyses we estimate the precision is ±0.2‰ for $\delta^{18}O$ and ±0.5‰ for $\delta^{2}H$.

2.4 Data processing and statistical analyses

We performed all data processing and statistical analyses with RStudio 1.1.383 (RStudio Inc., Boston, Massachusetts, USA) using R 3.4.2 (R Foundation for Statistical Computing, Vienna, Austria). Averaged data and variance in figures and tables are shown as mean ± standard deviation. Significant differences were determined with the Kruskal-Wallis test ($\alpha = 0.05$). We performed plots with *ggplot2*, *ggtern*, and *lattice* R packages, and used normality (eq L^{-1}) for the ternary diagram. Geographical maps were prepared using Quantum GIS 2.18 (Quantum GIS Development Team, 2017).

The Cryosphere Discuss., https://doi.org/10.5194/tc-2017-265
Manuscript under review for journal The Cryosphere
Discussion started: 12 December 2017

3 Results

3.1 Snowpack development and snowpack physics

Due to high wind conditions in the Arctic tundra (Cherry et al., 2014), the physical development of the snowpack and its depth and the thickness of wind slab layers at Toolik were subject to significant drifts and changes in snowpack height, and were hence highly variable spatially and temporally throughout the winter season. The average snow height over the tundra site (shown in gray bars in Figure 2) was continuously measured in both winters using a camera set to record daily pictures and using reference snow stakes placed in the snowpack. In the 2014–2015 season, the average snowpack height was 37 cm, with a standard deviation of 12 cm and a maximum depth of 60 cm. In the 2015–2016 season, the snowpack was almost half of that of the previous year, with an average snowpack height of 19 cm, a standard deviation of 7 cm, and a maximum depth of 35 cm. Based on snow pit measurements in the 2014–2015 season, we observed an increase of snow density with time, from an average of 0.18 g cm^{-3} in October to 0.26 g cm^{-3} in March (blue lines in Figure 2). No clear temporal pattern was observed in the 2015–2016 season when average snow density ranged between 0.28 and 0.30 g cm^{-3}. Snow water equivalent (SWE), which represents the amount of water stored in the snowpack, was calculated using snow density measurements in incremental 10 cm-layers, multiplied by snow height. Results showed similar temporal evolution as snow heights, with maximum SWE observed in March in both snow seasons of 158 and 116 mm, respectively.

Snowpack temperatures were highly variable throughout the seasons and also strongly differed vertically within the snowpack (red lines in Figure 2). Temperatures ranged from −34 to 0 °C in the top of the snowpack and from −21 to −1 °C in the bottom of the snowpack; temperatures always showed increases from the top to the bottom, illustrating the important insulating function that the snowpack has in the cold winter and spring months. Minimum snowpack temperatures were recorded during the January 26th 2015 sampling event when air temperatures were −40 °C.

The snowpack over the adjacent frozen lake showed an average density of 0.23 g cm^{-3} and temperatures ranged between −18 and 0 °C. The snow height over Toolik Lake was much lower than that over the tundra, with snow heights consistently <15 cm for both seasons. The maximum SWE calculated above the lake was 40 and 42 mm for the two snow seasons, respectively.

The transect between Toolik and the Arctic Ocean performed in March 2016 showed snowpack height ranging between 30 and 66 cm. The maximum height was observed 55 km from the Arctic Ocean (presence of dense shrubs up to 40 cm height). Snow density (between 0.19 and 0.26 g cm^{-3}) and temperatures (between −20 and −10 °C) followed the same trends as observed at Toolik with decreasing density and increasing temperatures with snowpack thickness. The calculated SWE averaged 104 mm and ranged between 70 and 164 mm.

3.2 Hg^0_{gas} in the atmosphere–snowpack–soil continuum

3.2.1 Hg^0_{gas} concentration profiles

Gaseous Hg^0 concentrations were measured at Toolik over two years in the atmosphere, in snowpack interstitial air at up to five inlet heights, and in soil pore air in the tundra ecosystem. Data coverage was 183 and 207 days for the 2014–2015 and

2015–2016 seasons, respectively, with only few periods when system failures resulted in lack of data. A continuous temporal record of Hg^0_{gas} concentration profile in the snowpack is presented for the 2014–2015 season, i.e., when the snowpack was deeper compared to the 2015–2016 season (Figure 3a), and compared to the literature from temperate snowpacks (Figure 3b; Faïn et al., 2013). The full time-averaged atmosphere–snowpack–soil Hg^0_{gas} diffusion profiles are shown for the two winter seasons: 2014–2015 (Figure 4a–c) and 2015–2016 (Figure 4d–f). For Figure 4, Hg^0_{gas} concentrations were averaged for each season for three different periods, i.e., November to December (representing early winter and full darkness), January to February (representing mid-winter and full darkness), and March to April (when sunlight emerged and when occasional AMDEs were active).

The Hg^0_{gas} measurements consistently showed strong concentration gradients in the atmosphere–snowpack–soil continuum with highest concentrations in the atmosphere (on average, 1.18 and 1.09 ng m^{-3}, respectively) and lowest concentrations in soils (mostly below the detection limits for both years, i.e., <0.05 ng m^{-3}). Hg^0_{gas} concentrations in the snowpack were in-between the two and showed pronounced patterns of decreasing concentrations from the top to the bottom of the snow profile. In the first year, Hg^0_{gas} concentrations decreased from the top snowpack inlet (i.e., 40 cm above the ground; average Hg^0_{gas} concentration of 1.18 ng m^{-3}) to the lower snowpack sampling heights (30, 20, and 10 cm above the ground; average Hg^0_{gas} concentrations of 1.11, 1.00, and 0.76 ng m^{-3}, respectively), and showed the lowest Hg^0_{gas} concentrations at the soil–snowpack interface (0 cm: 0.53 ng m^{-3}). Due to a much shallower snowpack in the 2015–2016 season and an absence of measurements at 0 cm height due to line freezing of the lowest inlet, the profile of Hg^0_{gas} was less pronounced compared to 2014–2015. However, we similarly found a Hg^0_{gas} decline from upper to lower snowpack heights (e.g., Hg^0_{gas} concentrations of 1.09 ng m^{-3} in the atmosphere, 1.02 ng m^{-3} at 20 cm, and 0.88 ng m^{-3} at 10 cm height above ground).

The top of the snowpack (between 2 and 12 cm from the atmosphere–snow interface) generally showed the highest Hg^0_{gas} concentrations that were close to ambient–air background concentrations measured in the atmosphere during most of the snow season. However, this pattern changed in March and April when atmospheric Hg^0_{gas} concentrations were highly variable as a result of ongoing AMDEs (Figure 4c and Figure 4f). During one of these periods shown in Figure S2, Hg^0_{gas} concentrations in the snowpack showed variable Hg^0_{gas} levels generally following Hg^0_{gas} concentration changes in the atmosphere above. During these time periods in March and April, snowpack Hg^0_{gas} concentrations in the top snowpack at times exceeded concentrations in the atmosphere above, as shown in Fig. S2. Periods when snowpack Hg^0_{gas} concentrations exceeded concentrations in the atmosphere occurred during less than 5% of the time and were mainly related to periods of AMDEs when Hg^0_{gas} depletion occurred in the overlying atmosphere.

Meanwhile, the soil pore air Hg^0_{gas} showed concentrations consistently below those measured in the snowpack (often below detection limits with an average concentration of 0.06 ng m^{-3}). Highest soil pore Hg^0_{gas} concentrations were measured in October and November for both years, after which soil pore Hg^0_{gas} concentrations declined and stayed mainly below the detection limits of our system (<0.05 ng m^{-3}) between December and May. This pattern was consistent for two independent soil profiles measured at this site, one mainly representing an organic soil profile and one profile dominated by mineral soil horizons.

The Cryosphere Discuss., https://doi.org/10.5194/tc-2017-265
Manuscript under review for journal The Cryosphere
Discussion started: 12 December 2017

3.2.2 Snowpack diffusivity of trace gases

We compared the ratios of Hg^0_{gas} to CO_2 gradients in the snowpack to determine commonality or differences between sinks and sources of both gases. Because CO_2 in the atmosphere is relatively stable in winter and soils are the only wintertime source, CO_2 can be used to assess how the snowpack affects diffusion and advective exchange processes between soils and the atmosphere. Comparing Hg^0_{gas} to CO_2 allows assessment of whether Hg^0_{gas} concentrations in the snowpack are driven by processes in the underlying soils (i.e., similar to CO_2) or if in-snowpack chemistry affects Hg^0_{gas} concentration profiles. The gas diffusion model, based on Fick's first law of diffusion, is defined as follows, Eq. (1):

$$F = -D\left(\frac{\delta C}{\delta z}\right) \quad (1)$$

where F is the molecular flux in the snowpack airspace (mol m^{-2} s^{-1}), D is the diffusivity in the snowpack airspace (m^2 s^{-1}), and $\delta C/\delta z$ is the gas concentration gradient in the snowpack integrated in the snow depth (mol m^{-4}).

Since diffusivity is determined by both snowpack porosity and tortuosity—both of which are poorly known and not directly measured—, we used the flux ratios between Hg^0_{gas} and CO_2 to determine if both gases show similar flux behavior across the snowpack (Faïn et al., 2013), Eq. (2):

$$\frac{F_{Hg^0{}_{gas}}}{F_{CO_2}} = \frac{D_{Hg^0{}_{gas}}}{D_{CO_2}} \times \frac{\Delta_{Hg^0{}_{gas}}}{\Delta_{CO_2}} \quad (2)$$

where $\Delta_{Hg^0{}_{gas}}$ and Δ_{CO_2} are the $\delta C/\delta z$ gradients for both Hg^0_{gas} and CO_2, respectively. Assuming similar gas diffusivity for both Hg^0_{gas} and CO_2, the ratio of concentration gradients of the two gases ($\Delta_{Hg^0{}_{gas}}/\Delta_{CO_2}$) gives direct information about their respective flux ratios between different snowpack trace gas inlets.

We focused our analysis of Hg^0_{gas} and CO_2 concentration gradients at Toolik for the month of January 2015 when the snow height was among the highest (approximatively 40 cm) and when strong decreases in interstitial Hg^0_{gas} concentrations from the top to the bottom of the snowpack were present. At this time, soils still were a relatively active source of CO_2 to the snowpack (Figure 5) facilitating a comparison to the soil CO_2 source. In contrast to Hg^0_{gas} (Figure 5a), profiles for CO_2 showed strong increases in concentrations with increasing depth in the snowpack (Figure 5b). Highest CO_2 concentrations were present in the soil (up to 5000 µmol mol^{-1}, data not shown), and these patterns are consistent with an expected source of soils for CO_2 and diffusive and advective mixing of CO_2 produced in snow through the snowpack with the atmosphere (Liptzin et al., 2009; Oechel et al., 1997). Analysis of $\Delta_{Hg^0{}_{gas}}/\Delta_{CO_2}$ ratios showed no statistically significant differences from the top to the bottom of the snowpack, as evidenced from calculated gradients between 0 to 10 cm, 10 to 20 cm, and 20 to 30 cm heights (Figure 5c).

3.3 Snowpack chemistry and snowbound mercury

3.3.1 Total and dissolved mercury concentrations

The Cryosphere Discuss., https://doi.org/10.5194/tc-2017-265
Manuscript under review for journal The Cryosphere
Discussion started: 12 December 2017

Snowpack and surface snow samples were analyzed at Toolik for Hg_{tot} and Hg_{diss} (Figure 2 and Table S1). Tundra snowpack averaged 0.70 ± 0.98 ng L^{-1} for Hg_{tot} concentrations and 0.17 ± 0.10 ng L^{-1} for Hg_{diss} concentrations (both seasons, average of entire snowpack height). Mercury content in the surface snow layer (top 3 cm only) averaged 0.53 ± 0.39 ng L^{-1} and 0.26 ± 0.26 ng L^{-1}, respectively, and was not statistically significantly different compared to that of full snow pits or bottom snow layers (averaging 0.49 ± 0.48 and 0.17 ± 0.12 ng L^{-1}). Total Hg and Hg_{diss} concentrations in the surface snow ranged from 0.18–1.46 and 0.04–1.15 ng L^{-1} most of the time, respectively (Table S1). The temporal pattern of Hg_{diss} concentrations of surface snow samples is reported in Figure 6. No consistent temporal trends in Hg_{tot} or Hg_{diss} were observed with increasing duration of winter in both seasons, and no correlations were observed with air temperatures (red line). One noticeable period of enhanced surface snow Hg concentrations was April 2016 when both Hg_{tot} and Hg_{diss} concentrations exceeded 1 ng L^{-1}, which was 4-times the average values observed through the rest of the season.

The snowpack sampled over the frozen lake showed Hg_{tot} and Hg_{diss} concentrations of 0.80 ± 0.61 and 0.15 ± 0.08 ng L^{-1}, respectively. Due to the low snow height on the frozen lake, we were able to collect only one depth sample per snow pit. Total Hg and Hg_{diss} concentrations of snow over the frozen lake were not statistically different in both seasons from concentrations measured in the tundra snowpack.

Measurements of Hg_{tot} and Hg_{diss} across a large North slope transect (about 200 km) in March, 2016 showed concentrations of 0.70 ± 0.79 and 0.24 ± 0.20 ng L^{-1}, respectively. Concentrations of Hg_{diss} of the five northernmost stations (<100 km distance from the Arctic Ocean) were statistically significantly ($p < 0.05$, Kruskal-Wallis test) higher compared to those measured in the four stations located in the interior tundra (>100 km) which included the Toolik site where the mean Hg_{diss} concentrations were 0.33 and 0.11 ng L^{-1} for the same period, respectively (Figure 7). It is noteworthy that no consistent vertical gradient concentrations were found in snow across the transect.

3.3.2 Cation and anion concentrations

Major cations and anions were measured in both snowpack and surface snow samples at Toolik (Table 1). Concentrations were comparable to other inland Alaskan sites and, similar to concentrations of Hg, were lower than data reported from several arctic coastal locations (de Caritat et al., 2005; Douglas and Sturm, 2004). Surface snow samples (top 3 cm) generally showed somewhat higher Cl^- and Na^+ concentrations and lower Mg^{2+} and K^+ concentrations than samples collected across the entire snowpack height, although only Mg^{2+} and Na^+ were significantly different ($p < 0.005$ and $p < 0.05$, respectively). Comparison between tundra and lake snowpack locations showed no statistical differences in elemental concentrations.

Spearman correlation coefficient (ρ) between Hg_{diss} and major ion concentrations were calculated for tundra and lake snowpack samples and surface snow collected over the tundra (Table 2). Using a correlation matrix, three groups of correlated major ions could be determined in the snowpack over the tundra: (1) NH_4^+ and SO_4^{2-}; (2) Ca^{2+}, Mg^{2+}, and NO_3^-; (3) Cl^-, K^+, and Na^+. In the tundra snowpack, Hg_{diss} was not statistically significantly ($-0.22 < \rho < 0.11$) correlated to any of these major ion groups when considering the entire depth of the tundra snowpack. Relationships, however, were present in surface snow over the tundra where Hg_{diss} was strongly correlated (ρ up to 0.80) with Ca^{2+}, Cl^-, and K^+. An additional group of correlated elements

was identified in surface snow samples: NH_4^+, NO_3^-, and SO_4^{2-}. The low number of lake snowpack samples (≤12) did not allow us to perform a meaningful correlation matrix analyses for lake snowpack samples.

To better visualize the relationships between analytes, we plotted a ternary diagram using three end-members according to Garbarino et al. (2002), Krnavek et al. (2012), Poulain et al. (2004), and Toom-Sauntry and Barrie (2002) (Figure 8). We considered Ca^{2+} as one end-member to represent a potential crustal signature, a second end-member with Cl^- as a sea salt signature, and a third end-member with SO_4^{2-} as a potential anthropogenic signature, i.e., from regional or long-range transport. Since sea salt SO_4^{2-} represented on average less than 1.2% of total SO_4^{2-} according to the calculation of Norman et al. (1999), we consider SO_4^{2-} not indicative of an ocean source. The different snow types (surface snow over the tundra, tundra snowpack, and lake snowpack) are presented with different colors in the Figure, and Hg_{diss} concentrations are represented by different symbol sizes. Relative contributions of Cl^- (i.e., sea salt influence) in samples showed statistically significant differences between tundra and lake locations (on average, 14 and 24% of proportion based on normality data, respectively; $p < 0.05$), but no statistically significant differences were observed for Ca^{2+} and SO_4^{2-}. In general, snow surface samples showed very low SO_4^{2-} and Cl^- relative concentrations (<30%) compared to integrated snowpack samples. Overall, Hg_{diss} concentrations were weakly correlated, except according to the SO_4^{2-} relative concentrations: Hg_{diss} concentrations averaged 0.10 and 0.17 ng L^{-1} for >30% and <30% of SO_4^{2-}, respectively ($p < 0.005$).

3.3.3 Oxygen and hydrogen isotope signatures

Oxygen (^{18}O) and hydrogen (^{2}H) isotopes are frequently used as tracers for precipitation sources (Gat, 2010). The isotope signatures in surface snow samples collected at Toolik are presented in a δ^2H vs $\delta^{18}O$ diagram for different ranges of Hg_{diss} concentrations and different sampling dates (Figure 9a). All the samples were distributed close to the global meteoritic water line (Craig, 1961). Despite a large variability in values (from −18.3 to −41.3‰ for $\delta^{18}O$ and from −140 to −314‰ for δ^2H), samples collected on the same date were relatively close (mean standard deviation of 0.88 and 6.5‰, respectively). No clear relationships were observed between isotope signatures and dissolved Hg concentrations (with size scale in Figure 9) across the entire spectrum of values. However, samples with high Hg_{diss} concentrations (e.g., the three highest measured in April 2nd, 2016) and low Hg_{diss} concentrations (e.g., samples below the detection limit in December 5th, 2015) were found clustered together at similar $\delta^{18}O$ and δ^2H values. The $\delta^{18}O$ values were also plotted against air temperatures (T_{air}) during the snowfall events (Figure 9b). A statistically significant linear relationship was found between the two variables ($r^2 = 0.50$) with the lowest $\delta^{18}O$ values being measured during the coldest temperatures.

4 Discussions

4.1 Gas-phase mercury exchanges in the snowpack and photochemical processes

The Cryosphere Discuss., https://doi.org/10.5194/tc-2017-265
Manuscript under review for journal The Cryosphere
Discussion started: 12 December 2017

We continuously measured Hg^0_{gas} concentrations and diffusion patterns in the atmosphere–snowpack–soil continuum throughout the two snow seasons at Toolik (Figure 3 and Figure 4). The measurement of trace gas concentration patterns allows determination of the direction of atmosphere-surface exchanges as trace gas exchange must follow concentration gradients (Sommerfeld et al., 1996). In a previous paper, we reported a small rate of continuous Hg^0_{gas} deposition from the atmosphere to the tundra—measured by a micrometeorological tower—during much of the snow-covered season, with the exception of short time periods in spring during the occurrence of AMDEs at Toolik (Obrist et al., 2017). Here, we show that these flux measurements are supported by consistent Hg^0_{gas} concentration gradients that existed through both seasons and that showed that snowpack Hg^0_{gas} concentrations were consistently lower than atmospheric levels in the snowpack. In addition, snowpack Hg^0_{gas} declined with depth in the snowpack and were lowest in the underlying soil, showing evidence of a consistent Hg^0_{gas} concentration gradient from the atmosphere to surface snow to tundra soils.

It is important to mention that our Hg^0_{gas} concentration profiles in the arctic snowpack are inherently different to patterns observed in lower latitude snowpacks. In the Rocky Mountains, for example, the upper snowpack showed strong enrichments of Hg^0_{gas} throughout most of the winter (i.e., up to 6-times higher concentrations than in the atmosphere; Figure 3b, Faïn et al., 2013). Such Hg^0_{gas} concentration enrichments were attributed to strong photochemically initiated reduction of snow-bound Hg^{II} to Hg^0_{gas} (Lalonde et al., 2002). The implications of Hg^0_{gas} production is that subsequent volatilization of the Hg^0_{gas} from the porous snowpack to the atmosphere can alleviate atmospheric deposition loads and it is estimated that globally 50% of snow-bound Hg is volatilized back to the atmosphere prior to snowmelt (Corbitt et al., 2011). Our trace gas concentration measurements showed that Hg^0_{gas} re-volatilization is missing in this interior tundra snowpack during most of the winter, and the absence of direct solar radiation likely explains the lack of photochemical Hg^0_{gas} formation and volatilization between December through mid-January. Yet, springtime is a photochemically active period in the arctic when strong Hg^0_{gas} volatilization from snow has been reported further north along the Arctic Ocean coast (Brooks et al., 2006; Kirk et al., 2006). Even in late spring, when abundant solar radiation is present, however, Hg^0_{gas} volatilization losses were rare and largely limited to periods of active AMDEs. We speculate that a reason for the general lack of Hg^0_{gas} formation and volatilization in snow includes substrate limitation due to very low total snow Hg concentrations (Figure 2, see below), several times lower compared to concentrations in temperate snowpacks (Faïn et al., 2013).

A key question pertaining to the wintertime Hg^0_{gas} concentration profiles and measured deposition is if the observed Hg^0_{gas} deposition and concentration declines in the snowpack are driven by Hg^0_{gas} sinks in the snowpack or by Hg^0_{gas} uptake by the underlying tundra. Sinks of Hg^0_{gas} in the snowpack have been observed in a few studies (Dommergue et al., 2003; Faïn et al., 2008, 2013) and attributed to dark oxidation of Hg^0_{gas} to divalent, non-volatile Hg^{II}, possibly including oxidation by halogen species, O_3, or related to NOx chemistry. To address this question, CO_2 serves as a tracer for soil contributions since soils are the only active wintertime sources of CO_2. Because the concentration gradients are directly related to the flux ratios, the consistent $\Delta_{Hg^0{}_{gas}}/\Delta_{CO_2}$ values through the snowpack provide evidence that the two trace gases are transported similarly

through the snowpack, although in opposite direction as shown by negative ratio values (Figure 5). This illustrates that the Hg^0_{gas} uptake occurs in soils rather than in the snowpack.

A soil Hg^0_{gas} sink was previously reported to occur in temperate soils (Obrist et al., 2014), although the mechanisms for the Hg^0_{gas} sinks are currently not clear. Our observations hence indicate that the tundra snowpack was not an active sink for atmospheric Hg^0_{gas}, but rather represented a porous and relatively unreactive matrix that reflected a strong concentration gradient between the atmosphere and tundra soils. The wintertime atmosphere–snowpack–soil Hg^0_{gas} concentration profiles at Toolik were consistent with a measured net deposition of Hg^0_{gas} throughout winter (Figure 2 and Figure 4; Obrist et al., 2017). Both net flux measurements and observations within the snowpack hence suggest that a soil Hg^0_{gas} sink was active throughout the Arctic winter, notably under very cold wintertime soil temperatures as low as −15 °C. It is notable that $\Delta_{Hg^0{}_{gas}}/\Delta_{CO_2}$ ratios in the upper snowpack (i.e., between 20 and 30 cm height) were more variable compared to lower snowpack heights, which we attribute to higher variability in upper snowpack concentrations due to variable atmospheric Hg^0_{gas} levels. Strong variations of Hg^0_{gas} concentrations were observed in the atmosphere—particularly during springtime (Figure S2)—, supporting the notion of snowpack as a highly porous matrix that is in strong diffusive and advective exchange with atmospheric trace gas concentrations (Figure 5).

Springtime was the only period when occasional Hg^0_{gas} concentration enhancements in the uppermost snowpack were present (less than 5% of the time) while deeper snowpack Hg^0_{gas} concentrations remained at low levels (Figure S2). Our measurements of Hg^0_{gas} showed that during March and April was the only time when we observed small rates of Hg^0_{gas} formation in the uppermost snowpack layer, suggesting some photochemical reduction and re-volatilization of Hg^0_{gas} after AMDE-Hg deposition. However, the Hg^0_{gas} production was small, limited in time, and no photochemical Hg^0_{gas} production and re-emission was observed from deeper snow layers suggesting that the process was limited to the snowpack surface. March and April were also the only months when we observed periods of net Hg^0_{gas} flux emission from the tundra ecosystem to the atmosphere (Obrist et al., 2017), in further support of the typical Hg dynamics reported during AMDEs (Hg^{II} deposition, photochemical reduction, Hg^0_{gas} re-emission; Ferrari et al., 2005). We propose that in addition to relatively weak and infrequent AMDE activity and Hg deposition in this interior arctic tundra, rapid photochemical re-emission losses of Hg following AMDEs render these events relatively unimportant as a deposition source of Hg. We provided support for this notion using stable Hg isotope analysis in soils from this site in Obrist et al. (2017) which showed that atmospheric Hg^0_{gas} is the dominant source to the interior tundra snowpack.

4.2 Spatial and temporal patterns of snowbound mercury in the interior arctic snowpack

Concentrations of Hg_{tot} and Hg_{diss} were measured in the snowpack overlying a tundra ecosystem at Toolik, a snowpack over the adjacent frozen Toolik Lake, and the tundra snowpack along a 170 km transect between Toolik and the Arctic Ocean (Figure 2, Figure 7, and Table S1). Total Hg concentrations in all snow samples collected (i.e., tundra snowpack, lake snowpack, and surface snow) were always much higher than Hg_{diss} levels, likely due to impurities and deposition of Hg

associated with plant detritus or soil dust. This also resulted in much higher variability of Hg_{tot} concentrations compared to Hg_{diss} concentrations. Due to the high variability in Hg_{tot} concentrations we focused our discussions on Hg_{diss} data. The measurements performed at Toolik showed low levels compared to many other high latitude studies, with Hg_{diss} concentrations averaging 0.17 ng L^{-1} and ranging between 0.08 and 1.15 ng L^{-1}, which is at the low end of concentration ranges reported in other studies mainly focused along the coastal zone (0.14–820 ng L^{-1} for both Hg_{diss} and Hg_{tot}; Douglas et al., 2005; Douglas and Sturm, 2004; Ferrari et al., 2004, 2005; Kirk et al., 2006; Nerentorp Mastromonaco et al., 2016; St. Louis et al., 2005; Steffen et al., 2002). The low concentrations we measured result in very small pool sizes of Hg_{diss} stored in the snowpack during wintertime compared to temperate studies (Pearson et al., 2015). At Toolik, snowpack pool sizes amounted to 26.9 and 19.7 ng m^{-2} during peak snowpack and prior to the onset of snowmelt in 2014–2015 and 2015–2016, respectively. Most other Arctic studies were performed close to the coast (i.e., Alert and Barrow), and few studies include inland sites such as Toolik (about 200 km south of the Arctic Ocean). Measurements performed along the transect across the Alaska North Slope (from Toolik to the Arctic Coast) in March 2016 indicated Hg_{diss} concentrations decreased significantly from the Arctic Ocean coast to inland (Figure 7). This is consistent with previous observations in Alaska in springtime that suggested an ocean influence on the presence of halogens in the coastal atmosphere resulting in higher Hg deposition (Douglas and Sturm, 2004; Landers et al., 1995; Snyder-Conn et al., 1997). We propose that low snowpack Hg concentrations (<0.5 ng L^{-1} for Hg_{diss}) are common in inland northern Alaska areas and that the interior arctic snowpacks exhibit lower levels compared to coastal locations that are subjected to a more significant ocean influences and impacts by AMDEs.

To our surprise, no consistent vertical patterns of Hg_{diss} concentrations were found in the snowpack at Toolik (Figure 2) and along the 200 km transect to the Arctic Coast (Figure 7). Thus, upper snowpack Hg_{diss} concentrations were not significantly different from those in the deeper layers, which is in contrast to patterns observed in the Sierra Nevada snowpack where strong concentration enhancements (i.e., more than 2-times the average snowpack concentrations (Faïn et al., 2011) were observed in the top 3 cm of the snowpack. This is likely due to lower atmospheric dry deposition inputs in this remote tundra atmosphere compared to more industrialized lower latitudes. Indeed, seasonal measurements at Toolik indicate a generic lack of atmospheric gaseous Hg^{II} during most of the year and very low amounts of total Hg^{II} deposition, i.e., wet, aerosols, plus gaseous Hg^{II} (Obrist et al., 2017). The lack of significant Hg^{II} dry deposition would prevent a Hg enhancement in surface snow and also is consistent with the low pool sizes of Hg in this tundra snowpack. Further support of this notion also includes that fresh snow collected at the surface throughout the arctic winter and spring was not statistically different from snow Hg concentrations contained in the entire snowpack (0.26 ± 0.26 vs 0.17 ± 0.10 ng L^{-1}, respectively). Yet, another factor to explain a lack of depth gradients in snow Hg concentrations may include that snow layers can be continuously mixed and redistributed by wind gust (e.g., >5 m s^{-1} 12% of the time) across the landscape in the Arctic (Cherry et al., 2014).

We observed significant differences in the amount of Hg contained in the snowpacks over the tundra and over the adjacent Toolik Lake. In fact, while Hg_{diss} concentrations were not statistically significantly different between tundra and lake snow (Table S1), snowpack Hg_{diss} loads on the frozen lake were much lower (6.2 ± 0.2 ng m^{-2}), i.e., only about ¼, compared to snowpack Hg_{diss} load on the adjacent tundra (23.3 ± 5.0 ng m^{-2}). Two reasons may explain the large discrepancy between lake

and tundra snowpack Hg loads: (1) lake would not accumulate the snowpack on open water prior to lake freezing in the early fall; (2) low surface roughness over the lake may prevent settling of snowfall and facilitate remobilization of snow by wind transport (Essery et al., 1999; Essery and Pomeroy, 2004). The implication of this process is a reduction of direct atmospheric deposition over Arctic lakes which is consistent with studies that estimated that annual Hg contribution to lakes via wet deposition is small, generally less than 20% of total deposition (Fitzgerald et al., 2005, 2014). Such spatial redistribution of snow across the tundra landscape further implies that both wet deposition and snow accumulation rates are variable leading to spatial heterogeneity of snowmelt Hg inputs.

Little temporal variation in snowpack Hg concentrations was observed between the early season snowpack evolving mainly under darkness and the late-season snowpack exposed to solar radiation (Figure 2 and Figure 6) although some temporal differences were evident during March and April when AMDEs were present in the region. Snowpack Hg_{diss} concentrations averaged 0.16 ng L^{-1} both during the completely dark period (i.e., December and January) and after March 1st. Such patterns support measurements of Hg^0_{gas} throughout the winter that indicated the snowpack to be a relatively inert matrix with little oxidoreduction reactions (oxidation of Hg^0_{gas} or reduction of Hg^{II}). An apparent trend in surface snow, however, emerged during springtime when Hg_{diss} concentrations reaching 1.15 ng L^{-1} were temporally measured in surface layers (Figure 6) in April 2016. This was a period when AMDEs occurred at this site, as evident by depletions of atmospheric Hg^0_{gas} with formation and deposition of oxidized atmospheric Hg^{II} (Obrist et al., 2017; Van Dam et al., 2013). Surface snow Hg concentration enhancements during AMDEs are commonly reported in polar regions, with at times Hg concentration enhancements up to 100-times the base concentration in the Arctic (Lalonde et al., 2002; Lindberg et al., 1998; Nerentorp Mastromonaco et al., 2016; Poulain et al., 2004; Steffen et al., 2002). The presence of AMDEs generally results in increased deposition of Hg to snow and ice surfaces, yet such additional deposition often is short-lived due to the photochemical re-emission of Hg^0_{gas} (Kirk et al., 2006). In our study, snow Hg_{diss} in surface snow quickly declined to levels similar to what was observed prior to AMDEs, and no corresponding concentration enhancements were observed deeper in the snowpack. The influence on snow Hg concentrations was therefore small compared to most studies reporting snow Hg enhancement during AMDEs. We attribute this to the large distance to the coast from our study site and the scarcity of AMDEs—and O_3 depletion events—that occur at this inland arctic location (Van Dam et al., 2013). Hence, minor impacts of AMDEs can be present in the interior arctic tundra as evident by patterns observed at Toolik some 200 km south of the Arctic Ocean.

Fresh surface snow that was collected throughout the season can serve as a proxy for atmospheric wet deposition Hg concentrations and loads (Faïn et al., 2011). Both low concentrations measured in fresh surface snow as well as low pool sizes as discussed above suggest low wet deposition rates during winter at our inland arctic sites. Estimation of deposition loads by snow collection can be compromised by quick re-volatilization losses of Hg from fresh snowfall (within the first few hours, e.g., Faïn et al., 2013), or snowmelt losses, but we do not consider these processes to be important at this site. The low Hg_{diss} concentrations measured in surface snow (0.26 ± 0.26 ng L^{-1}) be lower than the 10th percentile of wet deposition Hg concentrations reported for Kodiak Island in Alaska during the same period (National Atmospheric Deposition Program, 2017). For comparison, snowfall Hg_{diss} concentrations measured at Alert were between 100 and 200-times higher than in our

measurements (A. Steffen, personal communication). Using median concentrations in the surface snow multiplied by the amount of wet deposition for each snow-covered season, we estimated the Hg_{diss} load annually deposited by snowfall to 41.3 and 15.3 ng m^{-2} in the 2014–2015 and 2015–2016, respectively. This is up to 100-times lower than values recently provided from a coastal location 400 km northwest of our study site (Douglas et al., 2017) and up to 200-times lower than long-term measurements from Alert between 1998 and 2010 (A. Steffen, personal communication).

4.3 Origin of mercury in the interior arctic snowpack

Major cation (Ca^{2+}, K^+, Mg^{2+}, Na^+, and NH_4^+) and anion (Cl^-, NO_3^-, and SO_4^{2-}) values are used to assess the chemical composition and potential origins for Hg in the snowpack (Pearson et al., 2015; Table 1). Three main sources of major ions have been identified in snow deposition in North America by several authors (de Caritat et al., 2005; Krnavek et al., 2012; Poulain et al., 2004; Toom-Sauntry and Barrie, 2002): (1) marine with sea spray (associated with Na^+ and Cl^-); (2) lithogenic with rock and soil dust (associated with Ca^{2+} and Mg^{2+}); and (3) anthropogenic with long-range acid pollution (associated with NH_4^+ and SO_4^{2-}). Results of correlation matrices (Table 2**b**) indicated that Hg_{diss} in the fresh surface snow (i.e., top 3 cm) originated from a mix of natural sources, possibly linked to both mineral dust (Ca^{2+}) and sea spray (Cl^-). The correlation between Ca^{2+} and Cl^- ($\rho = 0.69$), as well as the absence of correlation between Hg_{diss} and Na^+ ($\rho = 0.30$), in surface snow samples likely indicated that a part of Cl^- was originated from mineral dust as $CaCl_2$. A minor influence of sea salt was consistent with coastal observations that showed the highest Hg concentrations close to the Arctic Ocean related to bromine chemistry (Figure 7; Douglas and Sturm, 2004). In addition, local or regional dust from rock and soil weathering contributed to the wintertime Hg deposition, particularly at the interior sites close to the Brooks Range where higher snow pH reported were from mineral dust that contained carbonates (Douglas and Sturm, 2004). Indeed, the mountain influence was dominant during the two snow-covered seasons at Toolik: 50% of snow events and 80% of dry periods (i.e., periods without snowfall, 90% of the time) coming from the south. Finally, the ternary diagram of major ions showed the highest Hg_{diss} concentrations were measured in snow with the lowest SO_4^{2-} (Figure 8), indicating that anthropogenic influence from combustion processes was minor or absent for snow Hg deposition. In fact, Alaska generally showed the lowest SO_4^{2-} concentrations among Arctic sites (de Caritat et al., 2005). Norman et al. (1999) also reported relatively small contributions of anthropogenic SO_4^{2-} in snow at Alert (Canada). From this, we propose that the Hg sources in the arctic snowpack is mainly derived from local lithological erosion, and that Arctic Ocean sources are minor contributions.

The lack of consistent statistically significant associations between major ions and Hg_{diss} across the entire snowpack depth (Table 2a) suggests that the original snowfall Hg content was maintained and largely unaltered after deposition, with no clear accumulation or depletion zones as found in other snowpacks (Ferrari et al., 2005; Poulain et al., 2004; Steffen et al., 2014). We found a small, relative enrichment of alkaline earth elements in snowpack samples compared to surface snow, which indicates some additional contributions of local mineral dust, yet this did not result in a measurable increase in snowpack Hg levels. Hence, we suggest no significant additional deposition of Hg (e.g., by dry deposition of gaseous or particulate Hg) to

exposed older snow consistent with the lack of correlation to pollution tracers (SO_4^{2-} and NO_3^-). We also suggest largely an absence of re-emission losses or elution losses from snow melt as occurs in temperate snowpacks (discussed in Faïn et al. (2013) and Pearson et al. (2015)). Elution losses are unlikely given that no temperatures above freezing were present in the Arctic until May, and atmospheric re-emissions losses of volatile Hg^0_{gas} were not important in this arctic snowpack for most of the season as discussed above.

Water stable isotope signatures in wet deposition indicated that some of the highest concentrations of Hg_{diss} (April 2016) were present when snow showed consistent values of δ^2H and $\delta^{18}O$ averaging −245.8 and −32.0‰, respectively (Figure 9). However, similar water isotope signatures were found also when Hg_{diss} concentrations were lower (e.g., November and December 2015), so that no significant associations of isotope signatures with Hg concentrations were found. Neither the origin of precipitation as shown by the wide range of isotope ratios, nor the physical conditions that often causes isotopic variation in precipitation (e.g., air temperatures that explain up to 50% of isotopic values via mass effects (Siegenthaler and Oeschger, 1980)), apparently shaped Hg concentrations in snow.

5 Conclusions

In this study, we investigated snow Hg dynamics in the interior arctic tundra at Toolik Field Station, Alaska, simultaneously analyzing Hg in: (1) the gas-phase (Hg^0_{gas}) of the atmosphere, interstitial snowpack, and soil pores; and (2) in the solid phase in snow (Hg_{tot} and Hg_{diss}). Gaseous Hg^0 in the atmosphere–snowpack–soil continuum showed consistent concentration patterns throughout most of the snow season, whereby the arctic tundra soil serves as a continuous sink for Hg^0_{gas}. To our surprise, photochemical formation of Hg^0_{gas} in the snowpack was largely absent and played a very minor role in the interior tundra largely limited to periods of active AMDEs. These observations are in contrast with strong photochemical formation of Hg^0_{gas} in surface snow observed at temperate sites and along the arctic coast resulting in significant photochemical losses of Hg^0_{gas} from these snowpacks. This calls for a regional adjustment of photochemical Hg^0_{gas} losses from the snowpack in models which should be treated differently in the arctic snowpack compared to temperate snowpacks. Small Hg_{diss} enhancements were temporarily observed in surface snow during springtime when AMDEs were present, reflecting the typical sequence of Hg deposition to the top snowpack followed by fast photochemical volatilization losses of Hg^0_{gas} during that time. At this interior arctic site, AMDEs, however, resulted in negligible deposition loads. Low concentrations of both Hg_{tot} and Hg_{diss} were measured in the snowpack across this northern Alaska region, resulting in a small reservoir of Hg stored in this snowpack available for potential mobilization during snowmelt (<30 ng m^{-2} for Hg_{diss}). These low values suggest that wet Hg deposition via snow is not a major source of Hg to this interior arctic site, a notion we previously supported by direct measurements and stable Hg isotopes that showed that two thirds of the Hg source are derived from Hg^0_{gas} deposition. Multielement analysis of fresh surface snow (top 3 cm) indicated that arctic snowpack Hg originated from a mix of diffuse and likely natural sources, including local mineral dust (associated with Ca^{2+} and Mg^{2+}) and, to a lesser extent, regional marine sea spray (associated with Cl^- and Na^+).

Acknowledgements

We thank Toolik Field Station staff for their support in this project over two years, especially Jeb Timm, Joe Franish, and Faye Ethridge for helping us with snow collection. We also thank Martin Jiskra (Geosciences Environnement Toulouse) and Christine Olson (DRI) for their field support, Christopher Pearson, Olivia Dillon, and Jacob Hoberg (DRI) for their support with laboratory analyses, and Dominique Colegrove and Tim Molnar (University of Colorado) for helping with field work and data processing. We finally thank Alexandra Steffen for providing mercury snow data from Alert. Funding was provided by the U.S. National Science Foundation (NSF) under award (#PLR 1304305).

References

Alaska Division of Oil and Gas: Regional geology of the north slope of Alaska, 2008.

Atwell, L., Hobson, K. A. and Welch, H. E.: Biomagnification and bioaccumulation of mercury in an arctic marine food web: insights from stable nitrogen isotope analysis, Can. J. Fish. Aquat. Sci., 55(5), 1114–1121, doi:10.1139/f98-001, 1998.

Bergin, M. H., Jaffrezo, J.-L., Davidson, C. I., Dibb, J. E., Pandis, S. N., Hillamo, R., Maenhaut, W., Kuhns, H. D. and Makela, T.: The contributions of snow, fog, and dry deposition to the summer flux of anions and cations at Summit, Greenland, J. Geophys. Res. Atmospheres, 100(D8), 16275–16288, doi:10.1029/95JD01267, 1995.

Brooks, S., Lindberg, S., Southworth, G. and Arimoto, R.: Springtime atmospheric mercury speciation in the McMurdo, Antarctica coastal region, Atmos. Environ., 42(12), 2885–2893, doi:10.1016/j.atmosenv.2007.06.038, 2008.

Brooks, S. B., Saiz-Lopez, A., Skov, H., Lindberg, S. E., Plane, J. M. C. and Goodsite, M. E.: The mass balance of mercury in the springtime arctic environment, Geophys. Res. Lett., 33(L13812), doi:10.1029/2005GL025525, 2006.

de Caritat, P., Hall, G., Gìslason, S., Belsey, W., Braun, M., Goloubeva, N. I., Olsen, H. K., Scheie, J. O. and Vaive, J. E.: Chemical composition of arctic snow: concentration levels and regional distribution of major elements, Sci. Total Environ., 336(1), 183–199, doi:10.1016/j.scitotenv.2004.05.031, 2005.

Cherry, J. E., Déry, S. J., Cheng, Y., Stieglitz, M., Jacobs, A. S. and Pan, F.: Climate and hydrometeorology of the Toolik Lake region and the Kuparuk River basin, in Alaska's changing arctic: ecological consequences for tundra, streams, and lakes, edited by J. E. Hobbie and G. W. Kling, pp. 21–60, Oxford University Press, New York., 2014.

Cobbett, F. D., Steffen, A., Lawson, G. and van Heyst, B. J.: GEM fluxes and atmospheric mercury concentrations (GEM, RGM and Hgp) in the Canadian Arctic at Alert, Nunavut, Canada (February–June 2005), Atmos. Environ., 41(31), 6527–6543, doi:10.1016/j.atmosenv.2007.04.033, 2007.

Corbitt, E. S., Jacob, D. J., Holmes, C. D., Streets, D. G. and Sunderland, E. M.: Global source-receptor relationships for mercury deposition under present-day and 2050 emissions scenarios, Environ. Sci. Technol., 45(24), 10477–10484, doi:10.1021/es202496y, 2011.

Craig, H.: Isotopic variations in meteoric waters, Science, 133(3465), 1702–1703, doi:10.1126/science.133.3465.1702, 1961.

Dominé, F. and Shepson, P. B.: Air-snow interactions and atmospheric chemistry, Science, 297(5586), 1506–1510, doi:10.1126/science.1074610, 2002.

Dommergue, A., Ferrari, C. P., Poissant, L., Gauchard, P.-A. and Boutron, C. F.: Diurnal cycles of gaseous mercury within the snowpack at Kuujjuarapik/Whapmagoostui, Québec, Canada, Environ. Sci. Technol., 37(15), 3289–3297, doi:10.1021/es026242b, 2003.

Dommergue, A., Sprovieri, F., Pirrone, N., Ebinghaus, R., Brooks, S., Courteaud, J. and Ferrari, C. P.: Overview of mercury measurements in the Antarctic troposphere, Atmospheric Chem. Phys., 10(7), 3309–3319, doi:10.5194/acp-10-3309-2010, 2010.

Douglas, T. A. and Sturm, M.: Arctic haze, mercury and the chemical composition of snow across northwestern Alaska, Atmos. Environ., 38(6), 805–820, doi:10.1016/j.atmosenv.2003.10.042, 2004.

Douglas, T. A., Sturm, M., Simpson, W. R., Brooks, S., Lindberg, S. E. and Perovich, D. K.: Elevated mercury measured in snow and frost flowers near Arctic sea ice leads, Geophys. Res. Lett., 32(4), L04502, doi:10.1029/2004GL022132, 2005.

Douglas, T. A., Sturm, M., Simpson, W. R., Blum, J. D., Alvarez-Aviles, L., Keeler, G. J., Perovich, D. K., Biswas, A. and Johnson, K.: Influence of snow and ice crystal formation and accumulation on mercury deposition to the Arctic, Environ. Sci. Technol., 42(5), 1542–1551, doi:10.1021/es070502d, 2008.

Douglas, T. A., Loseto, L. L., Macdonald, R. W., Outridge, P., Dommergue, A., Poulain, A., Amyot, M., Barkay, T., Berg, T., Chételat, J., Constant, P., Evans, M., Ferrari, C., Gantner, N., Johnson, M. S., Kirk, J., Kroer, N., Larose, C., Lean, D., Nielsen, T. G., Poissant, L., Rognerud, S., Skov, H., Sørensen, S., Wang, F., Wilson, S. and Zdanowicz, C. M.: The fate of mercury in arctic terrestrial and aquatic ecosystems, a review, Environ. Chem., 9(4), 321–355, doi:10.1071/EN11140, 2012.

Douglas, T. A., Sturm, M., Blum, J. D., Polashenski, C., Stuefer, S., Hiemstra, C., Steffen, A., Filhol, S. and Prevost, R.: A pulse of mercury and major ions in snowmelt runoff from a small arctic Alaska watershed, Environ. Sci. Technol., 51(19), 11145–11155, doi:10.1021/acs.est.7b03683, 2017.

Driscoll, C. T., Mason, R. P., Chan, H. M., Jacob, D. J. and Pirrone, N.: Mercury as a global pollutant: sources, pathways, and effects, Environ. Sci. Technol., 47(10), 4967–4983, doi:10.1021/es305071v, 2013.

Essery, R. and Pomeroy, J.: Vegetation and topographic control of wind-blown snow distributions in distributed and aggregated simulations for an arctic tundra basin, J. Hydrometeorol., 5(5), 735–744, doi:10.1175/1525-7541(2004)005<0735:VATCOW>2.0.CO;2, 2004.

Essery, R., Li, L. and Pomeroy, J.: A distributed model of blowing snow over complex terrain, Hydrol. Process., 13(1415), 2423–2438, doi:10.1002/(SICI)1099-1085(199910)13:14/15<2423::AID-HYP853>3.0.CO;2-U, 1999.

Faïn, X., Grangeon, S., Bahlmann, E., Fritsche, J., Obrist, D., Dommergue, A., Ferrari, C. P., Cairns, W., Ebinghaus, R., Barbante, C., Cescon, P. and Boutron, C.: Diurnal production of gaseous mercury in the alpine snowpack before snowmelt, J. Geophys. Res., 112(D21311), doi:10.1029/2007JD008520, 2007.

Faïn, X., Ferrari, C. P., Dommergue, A., Albert, M., Battle, M., Arnaud, L., Barnola, J.-M., Cairns, W., Barbante, C. and Boutron, C.: Mercury in the snow and firn at Summit Station, Central Greenland, and implications for the study of past atmospheric mercury levels, Atmos Chem Phys, 8(13), 3441–3457, doi:10.5194/acp-8-3441-2008, 2008.

Faïn, X., Obrist, D., Pierce, A., Barth, C., Gustin, M. S. and Boyle, D. P.: Whole-watershed mercury balance at Sagehen Creek, Sierra Nevada, CA, Geochim. Cosmochim. Acta, 75(9), 2379–2392, doi:10.1016/j.gca.2011.01.041, 2011.

Faïn, X., Helmig, D., Hueber, J., Obrist, D. and Williams, M. W.: Mercury dynamics in the Rocky Mountain, Colorado, snowpack, Biogeosciences, 10(6), 3793–3807, doi:10.5194/bg-10-3793-2013, 2013.

Ferrari, C. P., Dommergue, A., Boutron, C. F., Jitaru, P. and Adams, F. C.: Profiles of mercury in the snow pack at Station Nord, Greenland shortly after polar sunrise, Geophys. Res. Lett., 31(3), L03401, doi:10.1029/2003GL018961, 2004.

Ferrari, C. P., Gauchard, P.-A., Aspmo, K., Dommergue, A., Magand, O., Bahlmann, E., Nagorski, S., Temme, C., Ebinghaus, R., Steffen, A., Banic, C., Berg, T., Planchon, F., Barbante, C., Cescon, P. and Boutron, C. F.: Snow-to-air exchanges of mercury in an Arctic seasonal snow pack in Ny-Ålesund, Svalbard, Atmos. Environ., 39(39), 7633–7645, doi:10.1016/j.atmosenv.2005.06.058, 2005.

Ferrari, C. P., Padova, C., Faïn, X., Gauchard, P.-A., Dommergue, A., Aspmo, K., Berg, T., Cairns, W., Barbante, C., Cescon, P., Kaleschke, L., Richter, A., Wittrock, F. and Boutron, C.: Atmospheric mercury depletion event study in Ny-Ålesund (Svalbard) in spring 2005. Deposition and transformation of Hg in surface snow during springtime, Sci. Total Environ., 397(1–3), 167–177, doi:10.1016/j.scitotenv.2008.01.064, 2008.

Fitzgerald, W. F., Engstrom, D. R., Lamborg, C. H., Tseng, C.-M., Balcom, P. H. and Hammerschmidt, C. R.: Modern and historic atmospheric mercury fluxes in Northern Alaska: global sources and arctic depletion, Environ. Sci. Technol., 39(2), 557–568, doi:10.1021/es049128x, 2005.

Fitzgerald, W. F., Hammerschmidt, C. R., Engstrom, D. R., Balcom, P. H., Lamborg, C. H. and Tseng, C.-M.: Mercury in the Alaskan arctic, in Alaska's changing arctic: ecological consequences for tundra, streams, and lakes, edited by J. E. Hobbie and G. W. Kling, pp. 287–302, Oxford University Press, New York., 2014.

Garbarino, J. R., Snyder-Conn, E., Leiker, T. J. and Hoffman, G. L.: Contaminants in Arctic snow collected over Northwest Alaskan sea ice, Water. Air. Soil Pollut., 139(1–4), 183–214, doi:10.1023/A:1015808008298, 2002.

Gat, J. R.: Isotope hydrology: a study of the water cycle, World Scientific, London., 2010.

King, M. D. and Simpson, W. R.: Extinction of UV radiation in arctic snow at Alert, Canada (82°N), J. Geophys. Res. Atmospheres, 106(D12), 12499–12507, doi:10.1029/2001JD900006, 2001.

Kirk, J. L., St. Louis, V. L. and Sharp, M. J.: Rapid reduction and reemission of mercury deposited into snowpacks during atmospheric mercury depletion events at Churchill, Manitoba, Canada, Environ. Sci. Technol., 40(24), 7590–7596, doi:10.1021/es061299+, 2006.

Krnavek, L., Simpson, W. R., Carlson, D., Domine, F., Douglas, T. A. and Sturm, M.: The chemical composition of surface snow in the Arctic: Examining marine, terrestrial, and atmospheric influences, Atmos. Environ., 50(Supplement C), 349–359, doi:10.1016/j.atmosenv.2011.11.033, 2012.

Lalonde, J. D., Poulain, A. J. and Amyot, M.: The role of mercury redox reactions in snow on snow-to-air mercury transfer, Environ. Sci. Technol., 36(2), 174–178, doi:10.1021/es010786g, 2002.

Landers, D. H., Ford, J., Gubala, C., Monetti, M., Lasorsa, B. K. and Martinson, J.: Mercury in vegetation and lake sediments from the U.S. Arctic, Water. Air. Soil Pollut., 80(1–4), 591–601, doi:10.1007/BF01189711, 1995.

Lindberg, S. E., Hanson, P. J., Meyers, T. P. and Kim, K.-H.: Air/surface exchange of mercury vapor over forests—the need for a reassessment of continental biogenic emissions, Atmos. Environ., 32(5), 895–908, doi:10.1016/S1352-2310(97)00173-8, 1998.

Liptzin, D., Williams, M. W., Helmig, D., Seok, B., Filippa, G., Chowanski, K. and Hueber, J.: Process-level controls on CO_2 fluxes from a seasonally snow-covered subalpine meadow soil, Niwot Ridge, Colorado, Biogeochemistry, 95(1), 151–166, doi:10.1007/s10533-009-9303-2, 2009.

Mann, E., Meyer, T., Mitchell, C. P. J. and Wania, F.: Mercury fate in ageing and melting snow: development and testing of a controlled laboratory system, J. Environ. Monit., 13(10), 2695–2702, doi:10.1039/C1EM10297D, 2011.

Mann, E., Ziegler, S., Mallory, M. and O'Driscoll, N.: Mercury photochemistry in snow and implications for arctic ecosystems, Environ. Rev., 22(4), 331–345, doi:10.1139/er-2014-0006, 2014.

Mann, E. A., Mallory, M. L., Ziegler, S. E., Tordon, R. and O'Driscoll, N. J.: Mercury in Arctic snow: quantifying the kinetics of photochemical oxidation and reduction, Sci. Total Environ., 509–510, 115–132, doi:10.1016/j.scitotenv.2014.07.056, 2015.

Monson, R. K., Burns, S. P., Williams, M. W., Delany, A. C., Weintraub, M. and Lipson, D. A.: The contribution of beneath-snow soil respiration to total ecosystem respiration in a high-elevation, subalpine forest, Glob. Biogeochem. Cycles, 20(GB3030), doi:10.1029/2005GB002684, 2006.

Moore, C. W., Obrist, D., Steffen, A., Staebler, R. M., Douglas, T. A., Richter, A. and Nghiem, S. V.: Convective forcing of mercury and ozone in the Arctic boundary layer induced by leads in sea ice, Nature, 506(7486), 81–84, doi:10.1038/nature12924, 2014.

National Atmospheric Deposition Program: (NRSP-3), NADP Program Office, Illinois State Water Survey, University of Illinois, Champaign, IL 61820., 2017.

Nerentorp Mastromonaco, M., Gårdfeldt, K., Jourdain, B., Abrahamsson, K., Granfors, A., Ahnoff, M., Dommergue, A., Méjean, G. and Jacobi, H.-W.: Antarctic winter mercury and ozone depletion events over sea ice, Atmos. Environ., 129, 125–132, doi:10.1016/j.atmosenv.2016.01.023, 2016.

Norman, A. L., Barrie, L. A., Toom-Sauntry, D., Sirois, A., Krouse, H. R., Li, S. M. and Sharma, S.: Sources of aerosol sulphate at Alert: apportionment using stable isotopes, J. Geophys. Res. Atmospheres, 104(D9), 11619–11631, doi:10.1029/1999JD900078, 1999.

Obrist, D., Tas, E., Peleg, M., Matveev, V., Faïn, X., Asaf, D. and Luria, M.: Bromine-induced oxidation of mercury in the mid-latitude atmosphere, Nat. Geosci., 4(1), 22–26, doi:10.1038/ngeo1018, 2011.

Obrist, D., Pokharel, A. K. and Moore, C.: Vertical profile measurements of soil air suggest immobilization of gaseous elemental mercury in mineral soil, Environ. Sci. Technol., 48(4), 2242–2252, doi:10.1021/es4048297, 2014.

Obrist, D., Agnan, Y., Jiskra, M., Olson, C. L., Colegrove, D. P., Hueber, J., Moore, C. W., Sonke, J. E. and Helmig, D.: Tundra uptake of atmospheric elemental mercury drives Arctic mercury pollution, Nature, 547(7662), 201–204, doi:10.1038/nature22997, 2017.

Oechel, W. C., Vourlitis, G. and Hastings, S. J.: Cold season CO_2 emission from arctic soils, Glob. Biogeochem. Cycles, 11(2), 163–172, doi:10.1029/96GB03035, 1997.

Pearson, C., Schumer, R., Trustman, B. D., Rittger, K., Johnson, D. W. and Obrist, D.: Nutrient and mercury deposition and storage in an alpine snowpack of the Sierra Nevada, USA, Biogeosciences, 12(12), 3665–3680, doi:10.5194/bg-12-3665-2015, 2015.

Poulain, A. J., Lalonde, J. D., Amyot, M., Shead, J. A., Raofie, F. and Ariya, P. A.: Redox transformations of mercury in an Arctic snowpack at springtime, Atmos. Environ., 38(39), 6763–6774, doi:10.1016/j.atmosenv.2004.09.013, 2004.

Schroeder, W. H. and Munthe, J.: Atmospheric mercury—An overview, Atmos. Environ., 32(5), 809–822, doi:10.1016/S1352-2310(97)00293-8, 1998.

Schroeder, W. H., Anlauf, K. G., Barrie, L. A., Lu, J. Y., Steffen, A., Schneeberger, D. R. and Berg, T.: Arctic springtime depletion of mercury, Nature, 394, 331–332, doi:10.1038/28530, 1998.

Selin, N. E.: Global biogeochemical cycling of mercury: a review, Annu. Rev. Environ. Resour., 34(1), 43–63, doi:10.1146/annurev.environ.051308.084314, 2009.

Seok, B., Helmig, D., Williams, M. W., Liptzin, D., Chowanski, K. and Hueber, J.: An automated system for continuous measurements of trace gas fluxes through snow: an evaluation of the gas diffusion method at a subalpine forest site, Niwot Ridge, Colorado, Biogeochemistry, 95(1), 95–113, doi:10.1007/s10533-009-9302-3, 2009.

Shaver, G. R. and Chapin, F. S.: Production: biomass relationships and element cycling in contrasting arctic vegetation types, Ecol. Monogr., 61(1), 1–31, doi:10.2307/1942997, 1991.

Siegenthaler, U. and Oeschger, H.: Correlation of ^{18}O in precipitation with temperature and altitude, Nature, 285(5763), 314–317, doi:10.1038/285314a0, 1980.

Simpson, W. R., von Glasow, R., Riedel, K., Anderson, P., Ariya, P., Bottenheim, J., Burrows, J., Carpenter, L. J., Frieß, U., Goodsite, M. E., Heard, D., Hutterli, M., Jacobi, H.-W., Kaleschke, L., Neff, B., Plane, J., Platt, U., Richter, A., Roscoe, H., Sander, R., Shepson, P., Sodeau, J., Steffen, A., Wagner, T. and Wolff, E.: Halogens and their role in polar boundary-layer ozone depletion, Atmos Chem Phys, 7(16), 4375–4418, doi:10.5194/acp-7-4375-2007, 2007.

Snyder-Conn, E., Garbarino, J. R., Hoffman, G. L. and Oelkers, A.: Soluble trace elements and total mercury in arctic alaskan snow, Arctic, 50(3), 201–215, 1997.

Sommerfeld, R. A., Massman, W. J., Musselman, R. C. and Mosier, A. R.: Diffusional flux of CO_2 through snow: spatial and temporal variability among alpine-subalpine sites, Glob. Biogeochem. Cycles, 10(3), 473–482, doi:10.1029/96GB01610, 1996.

Sprovieri, F., Pirrone, N., Ebinghaus, R., Kock, H. and Dommergue, A.: A review of worldwide atmospheric mercury measurements, Atmospheric Chem. Phys., 10(17), 8245–8265, doi:10.5194/acp-10-8245-2010, 2010.

St. Louis, V. L., Sharp, M. J., Steffen, A., May, A., Barker, J., Kirk, J. L., Kelly, D. J. A., Arnott, S. E., Keatley, B. and Smol, J. P.: Some sources and sinks of monomethyl and inorganic mercury on Ellesmere Island in the Canadian high Arctic, Environ. Sci. Technol., 39(8), 2686–2701, doi:10.1021/es049326o, 2005.

Steffen, A., Schroeder, W., Bottenheim, J., Narayan, J. and Fuentes, J. D.: Atmospheric mercury concentrations: measurements and profiles near snow and ice surfaces in the Canadian Arctic during Alert 2000, Atmos. Environ., 36(15–16), 2653–2661, doi:10.1016/S1352-2310(02)00112-7, 2002.

Steffen, A., Douglas, T., Amyot, M., Ariya, P., Aspmo, K., Berg, T., Bottenheim, J., Brooks, S., Cobbett, F., Dastoor, A., Dommergue, A., Ebinghaus, R., Ferrari, C., Gardfeldt, K., Goodsite, M. E., Lean, D., Poulain, A. J., Scherz, C., Skov, H., Sommar, J. and Temme, C.: A synthesis of atmospheric mercury depletion event chemistry in the atmosphere and snow, Atmos Chem Phys, 8(6), 1445–1482, doi:10.5194/acp-8-1445-2008, 2008.

Steffen, A., Bottenheim, J., Cole, A., Douglas, T. A., Ebinghaus, R., Friess, U., Netcheva, S., Nghiem, S., Sihler, H. and Staebler, R.: Atmospheric mercury over sea ice during the OASIS-2009 campaign, Atmospheric Chem. Phys., 13(14), 7007–7021, doi:10.5194/acp-13-7007-2013, 2013.

Steffen, A., Bottenheim, J., Cole, A., Ebinghaus, R., Lawson, G. and Leaitch, W. R.: Atmospheric mercury speciation and mercury in snow over time at Alert, Canada, Atmos Chem Phys, 14(5), 2219–2231, doi:10.5194/acp-14-2219-2014, 2014.

Toom-Sauntry, D. and Barrie, L. A.: Chemical composition of snowfall in the high Arctic: 1990–1994, Atmos. Environ., 36(15–16), 2683–2693, doi:10.1016/S1352-2310(02)00115-2, 2002.

Uematsu, M., Kinoshita, K. and Nojiri, Y.: Scavenging of insoluble particles from the marine atmosphere over the sub-arctic north Pacific, J. Atmospheric Chem., 35(2), 151–163, doi:10.1023/A:1006219028497, 2000.

US EPA: Method 1631: Mercury in water by oxidation, purge and trap, and cold vapor atomic fluorescence spectrometry, United States Environmental Protection Agency., 2002.

Van Dam, B., Helmig, D., Burkhart, J. F., Obrist, D. and Oltmans, S. J.: Springtime boundary layer O_3 and GEM depletion at Toolik Lake, Alaska, J. Geophys. Res. Atmospheres, 118(8), 3382–3391, doi:10.1002/jgrd.50213, 2013.

The Cryosphere Discuss., https://doi.org/10.5194/tc-2017-265
Manuscript under review for journal The Cryosphere
Discussion started: 12 December 2017

Table 1: Mean concentration (µg L^{-1}), including standard deviation (italic), of cations and anions in the collected snow precipitation and both tundra and lake snowpack at Toolik Field Station.

location		Mg^{2+}	Ca^{2+}	Na^{+}	K^{+}	Cl^{-}	NH_4^{+}	NO_3^{-}	SO_4^{2-}
tundra	surface	7.2	453.0	112.6	29.4	228.6	11.3	265.0	191.3
		6.8	*530.8*	*104.6*	*46.7*	*232.9*	*3.9*	*187.5*	*130.6*
	snowpack	32.1	523.5	58.5	60.8	137.5	13.2	202.8	234.0
		34.7	*452.1*	*38.9*	*102.3*	*113.1*	*5.4*	*104.5*	*131.8*
lake		27.8	784.1	119.1	23.1	117.5	12.8	270.5	181.2
		21.8	*403.7*	*135.9*	*28.6*	*73.4*	*2.9*	*94.0*	*78.1*

The Cryosphere Discuss., https://doi.org/10.5194/tc-2017-265
Manuscript under review for journal The Cryosphere
Discussion started: 12 December 2017

Table 2: Spearman's coefficient correlations (ρ, in bold if ≥0.5 or ≤−0.5) between chemical elements (dissolved Hg [Hg_{diss}] and major ions) in the tundra snowpack (a) and surface snow over the tundra (b).

a. Tundra snowpack

	Hg_{diss}	Mg^{2+}	Ca^{2+}	Na^{+}	K^{+}	Cl^{-}	NH_4^{+}	NO_3^{-}
SO_4^{2-}	−0.16	0.42	0.32	0.39	0.48	0.47	**0.58**	0.17
NO_3^{-}	0.07	**0.74**	**0.83**	**0.55**	0.33	**0.59**	0.03	
NH_4^{+}	−0.22	−0.04	0.03	0.15	0.35	0.30		
Cl^{-}	−0.11	0.41	0.39	**0.89**	**0.72**			
K^{+}	−0.10	0.34	0.33	**0.70**				
Na^{+}	0.11	0.47	0.38					
Ca^{2+}	−0.07	**0.90**						
Mg^{2+}	0.06							

b. Surface snow

	Hg_{diss}	Mg^{2+}	Ca^{2+}	Na^{+}	K^{+}	Cl^{-}	NH_4^{+}	NO_3^{-}
SO_4^{2-}	−0.08	**0.54**	0.14	0.16	−0.08	−0.04	**0.74**	**0.74**
NO_3^{-}	0.14	**0.62**	0.28	0.08	0.07	−0.20	**0.57**	
NH_4^{+}	−0.02	0.45	0.24	0.18	−0.08	−0.04		
Cl^{-}	**0.63**	0.35	**0.69**	**0.82**	**0.86**			
K^{+}	**0.62**	0.45	**0.80**	**0.78**				
Na^{+}	0.30	**0.68**	**0.56**					
Ca^{2+}	**0.80**	0.39						
Mg^{2+}	0.08							

The Cryosphere Discuss., https://doi.org/10.5194/tc-2017-265
Manuscript under review for journal The Cryosphere
Discussion started: 12 December 2017

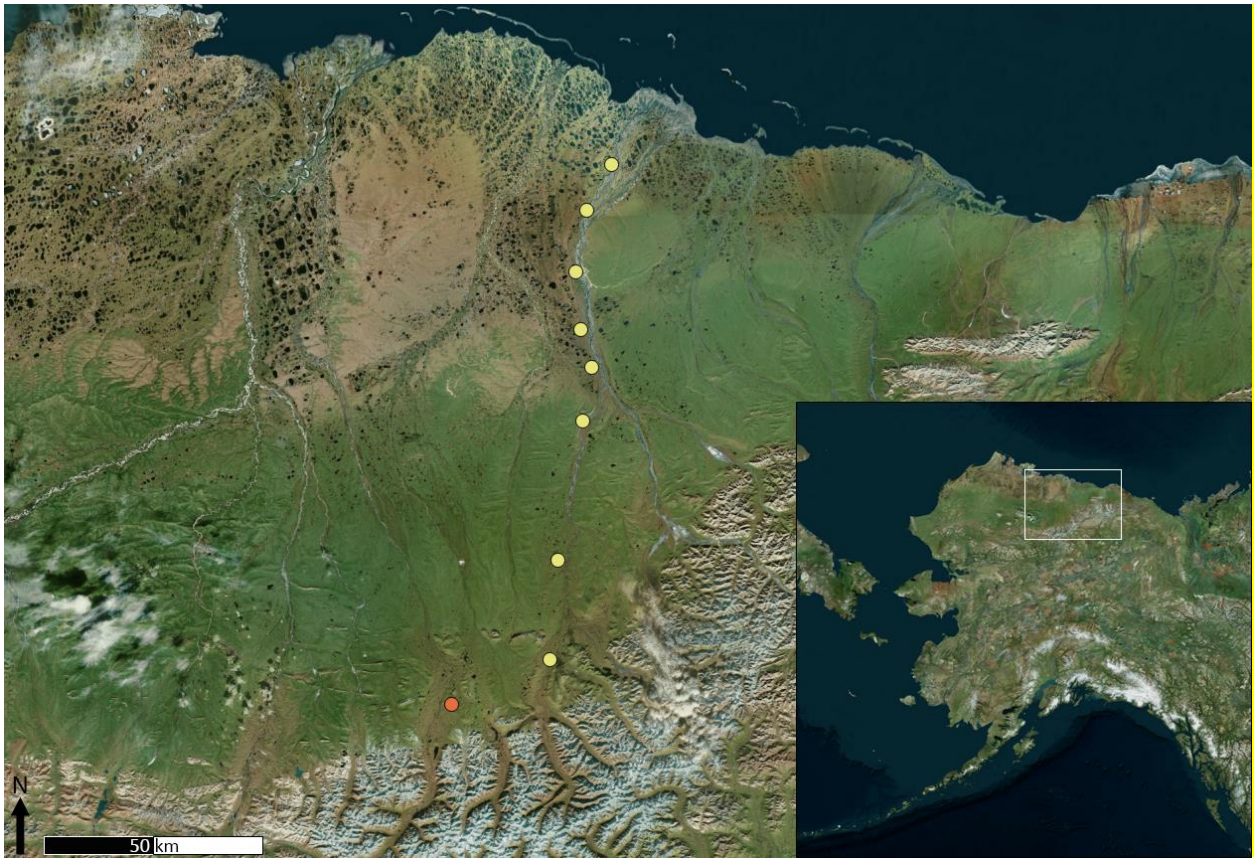

Figure 1: Study area in northern Alaska, including Toolik Field Station (orange bullet point) and the eight transect sites (yellow bullet points). Satellite images are true color images (Earthstar Geographics SIO, 2017).

The Cryosphere Discuss., https://doi.org/10.5194/tc-2017-265
Manuscript under review for journal The Cryosphere
Discussion started: 12 December 2017

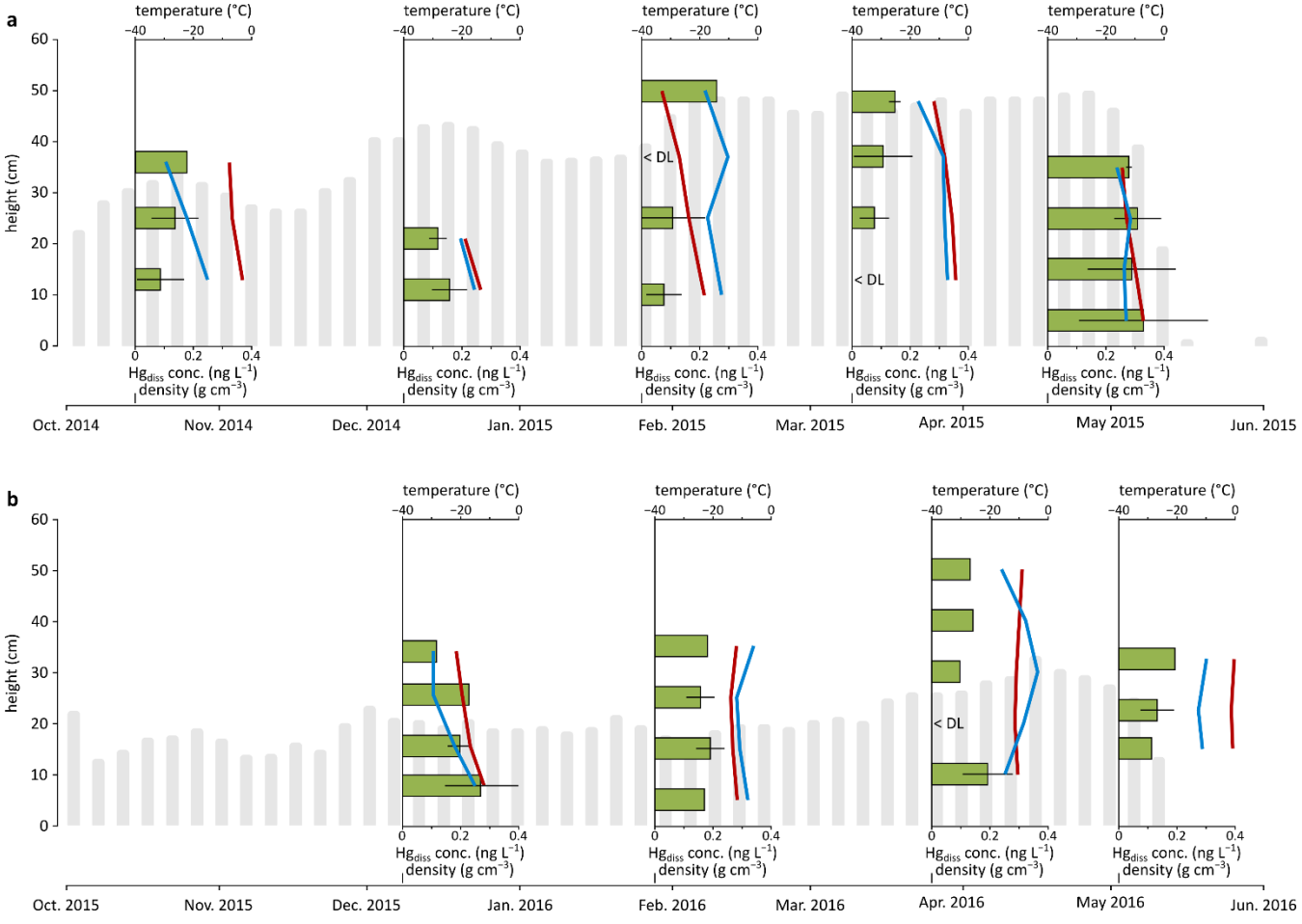

Figure 2: Snowpack temperatures (red lines) and densities (blue lines) and dissolved Hg concentrations (green bars, including mean values and standard deviations) for five snow pits in the 2014–2015 season (a) and four snow pits in the 2015–2016 season (b) over the Arctic tundra at Toolik Field Station. The gray bars illustrate the average snow heights.

The Cryosphere Discuss., https://doi.org/10.5194/tc-2017-265
Manuscript under review for journal The Cryosphere
Discussion started: 12 December 2017

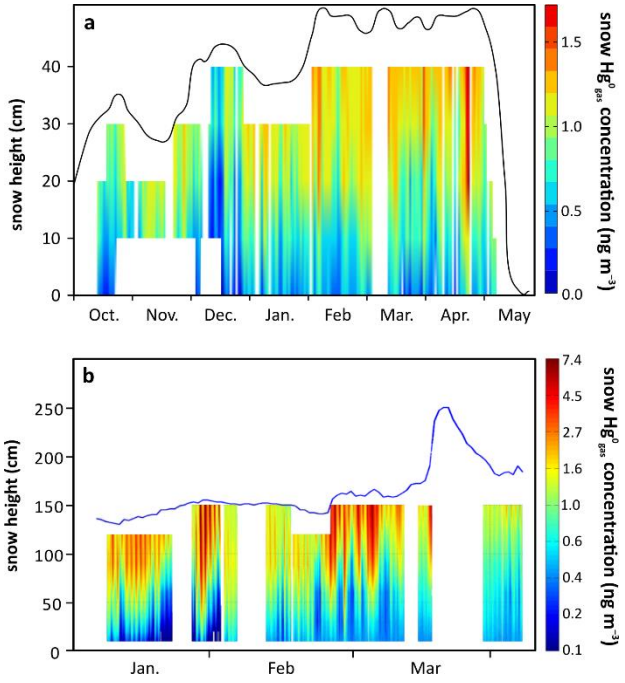

Figure 3: Gaseous Hg^0 concentration profiles in the snowpack interstitial air during the snow-covered season from October 2014 to May 2015 over the Arctic tundra measured at Toolik Field Station based on continuous observations at up to five heights in the snowpack each hour, and interpolation of this data across the entire snowpack (a). For comparison, interpolated Hg^0_{gas} concentration profiles in snowpack interstitial air during the snow-covered season based on similar measurements at Niwot Ridge, Rocky Mountains, Colorado, USA, during the winter of 2009 (b) (adapted with permission; Faïn et al., 2013).

The Cryosphere Discuss., https://doi.org/10.5194/tc-2017-265
Manuscript under review for journal The Cryosphere
Discussion started: 12 December 2017

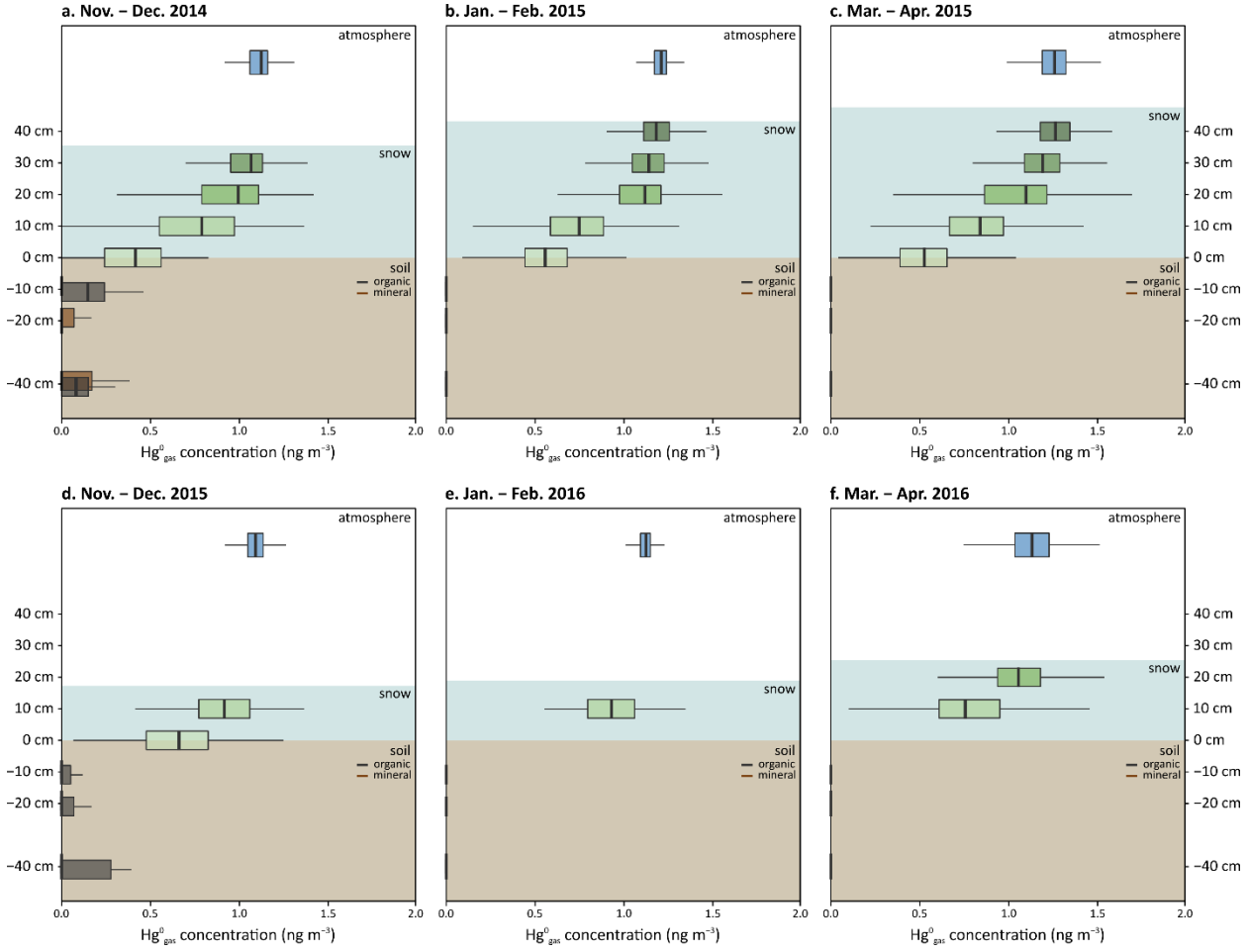

Figure 4: Hg^0_{gas} concentration profiles in the atmosphere, snowpack interstitial air, and soil interstitial air in early winter (from November to December; a and d), in winter (from January to February; b and e), and in early spring (from March to April; c and f) for 2014–2015 (top panels) and 2015–2016 (bottom panels) snow-covered periods over the arctic tundra measured at Toolik Field Station.

The Cryosphere Discuss., https://doi.org/10.5194/tc-2017-265
Manuscript under review for journal The Cryosphere
Discussion started: 12 December 2017

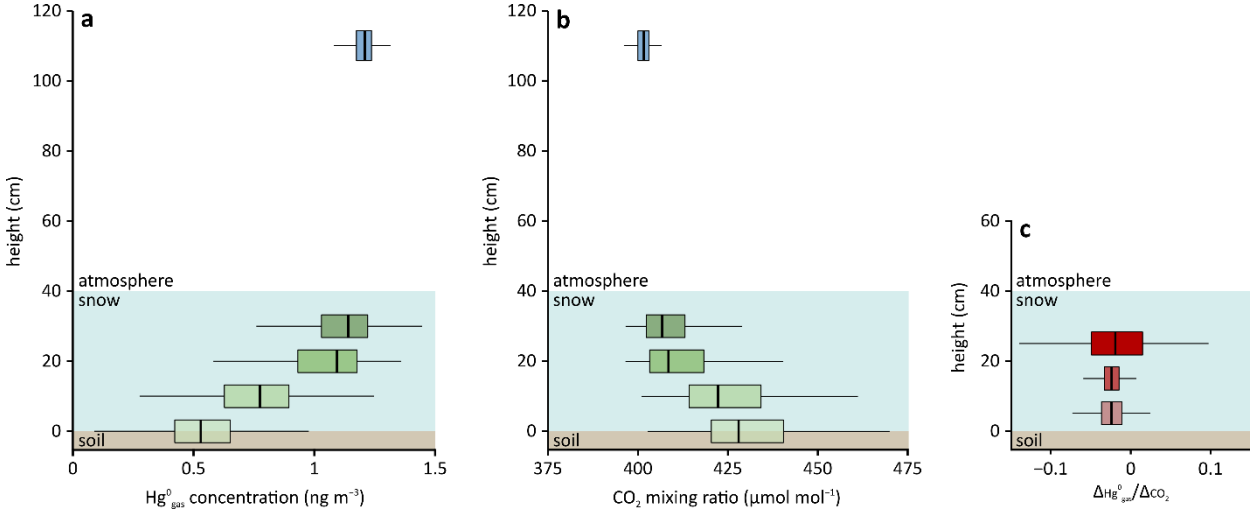

Figure 5: Snow concentration profiles for Hg^0_{gas} (a) and CO_2 (b) concentrations and $\Delta_{Hg^0_{gas}}/\Delta_{CO_2}$ ratios for 0 to 10 cm, 10 to 20 cm, and 20 to 30 cm snowpack height (c) in January 2015 (snow height averaged 40 cm) over the arctic tundra measured at Toolik Field Station.

The Cryosphere Discuss., https://doi.org/10.5194/tc-2017-265
Manuscript under review for journal The Cryosphere
Discussion started: 12 December 2017

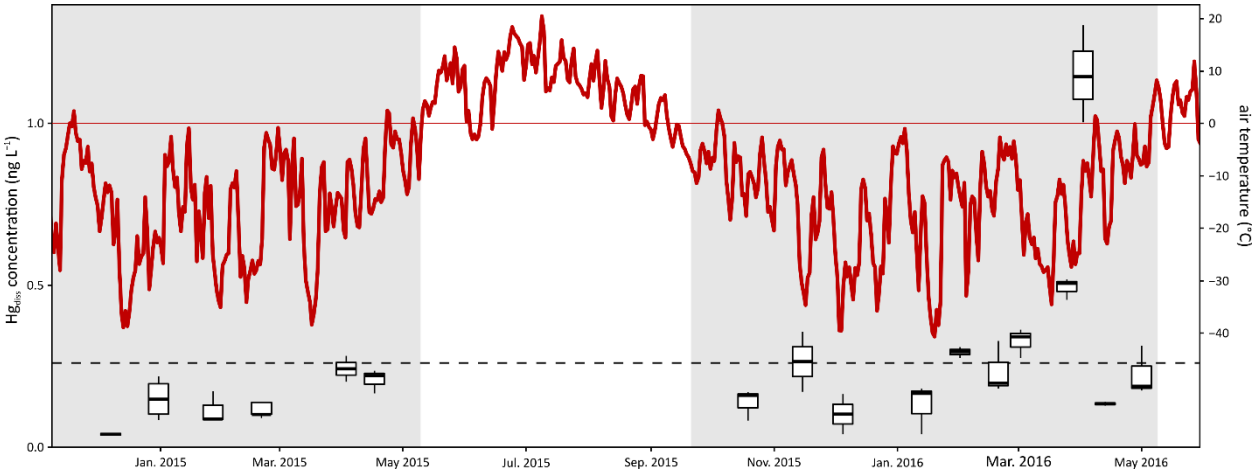

Figure 6: Temporal pattern of dissolved Hg (Hg_{diss}) concentrations in surface snow samples (top 3 cm) throughout the 2014–2015 and 2015–2016 snow-covered seasons (in grey) at Toolik Field Station. The broken line indicates the average surface snow Hg_{diss} concentration (0.26 ng L^{-1}). The red line indicates the daily average air temperature.

The Cryosphere Discuss., https://doi.org/10.5194/tc-2017-265
Manuscript under review for journal The Cryosphere
Discussion started: 12 December 2017

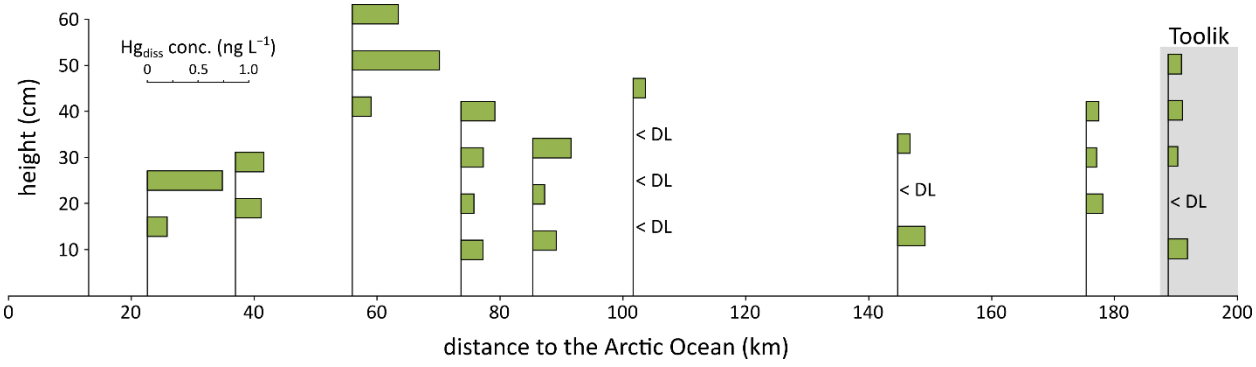

Figure 7: Spatial pattern of dissolved Hg concentrations (Hg_{diss}) in snowpack profiles across the North slope transect on March 27th–28th, 2016, and comparison with Toolik Field Station (gray box) in March 25th, 2016.

The Cryosphere Discuss., https://doi.org/10.5194/tc-2017-265
Manuscript under review for journal The Cryosphere
Discussion started: 12 December 2017

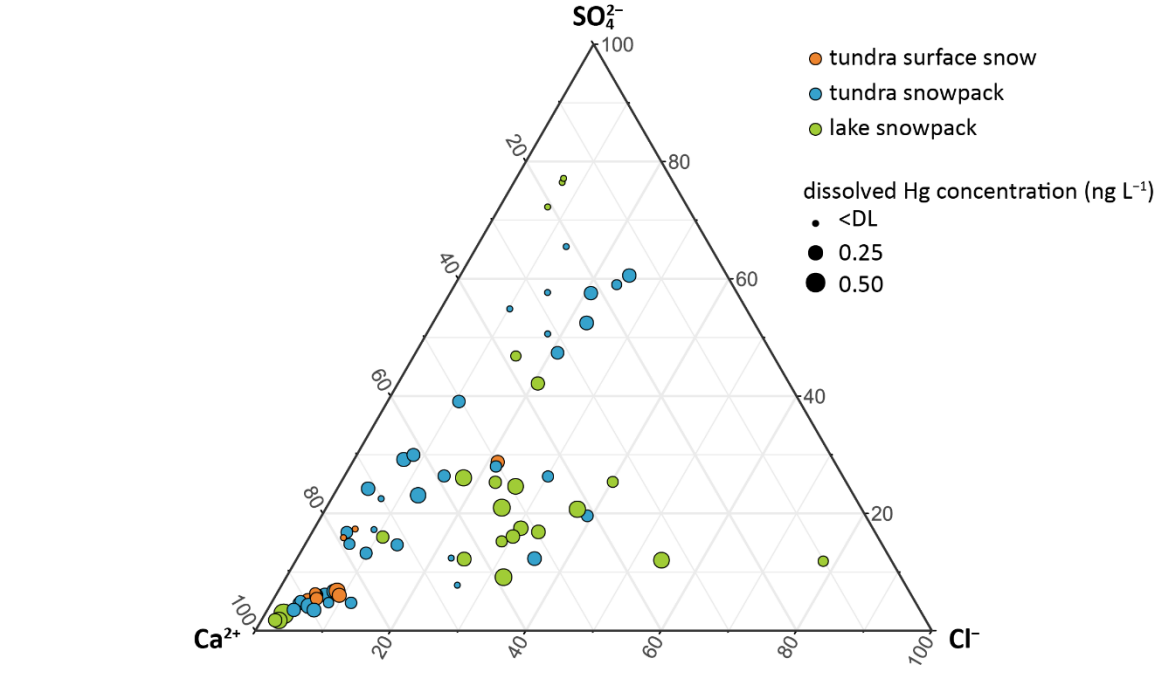

Figure 8: Ternary diagram of tundra surface snow (orange), tundra snowpack (blue), and lake snowpack (green) samples from Toolik Field Station ordered by dissolved Hg concentration between Ca^{2+}, Cl^-, and SO_4^{2-} (proportions based on meq L^{-1}).

The Cryosphere Discuss., https://doi.org/10.5194/tc-2017-265
Manuscript under review for journal The Cryosphere
Discussion started: 12 December 2017

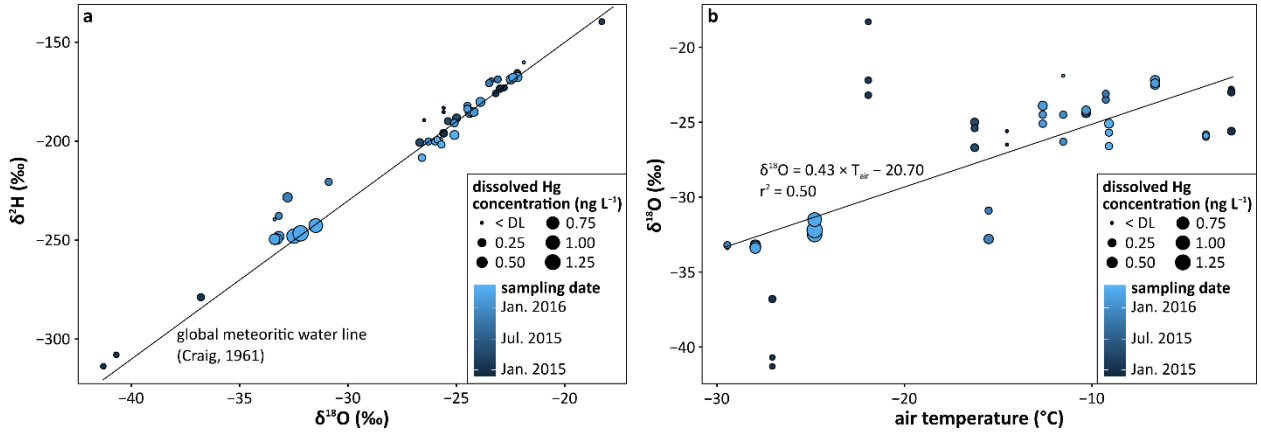

Figure 9: Dissolved Hg concentrations in surface snow samples for 2014 to 2016 in: (a) the δ^2H vs $\delta^{18}O$ diagram and (b) a plot of $\delta^{18}O$ vs air temperature (T_{air}) during the previous snowfall at Toolik Field Station.